NBSIR 74-474

Metallurgical Analysis of Wear Particles and Wearing Surfaces

A. W. Ruff

Metallurgy Division
Institute for Materials Research
National Bureau of Standards
Washington, D. C. 20234

April 1974

Final Report
NAONR-31-73
NR 229-014

Prepared for

Department of the Navy
Office of Naval Research
Arlington, Virginia 22217
Naval Air Engineering Center
Philadelphia, Pa. 19112

NBSIR 74-474

METALLURGICAL ANALYSIS OF WEAR PARTICLES AND WEARING SURFACES

A. W. Ruff

Metallurgy Division
Institute for Materials Research
National Bureau of Standards
Washington, D. C. 20234

April 1974

Final Report
NAONR-31-73
NR 229-014

Prepared for
Department of the Navy
Office of Naval Research
Arlington, Virginia 22217
Naval Air Engineering Center
Philadelphia, Pa. 19112

U. S. DEPARTMENT OF COMMERCE, Frederick B. Dent, Secretary
NATIONAL BUREAU OF STANDARDS, Richard W. Roberts, Director

Unclassified

Security Classification

DOCUMENT CONTROL DATA - R & D

(Security classification of title, body of abstract and indexing annotation must be entered when the overall report is classified)

1. ORIGINATING ACTIVITY (Corporate author)

National Bureau of Standards
Washington, D. C. 20234
Attn: A. W. Ruff, Metallurgy Division

2a. REPORT SECURITY CLASSIFICATION

Unclassified

2b. GROUP

3. REPORT TITLE

METALLURGICAL ANALYSIS OF WEAR PARTICLES AND WEARING SURFACES

4. DESCRIPTIVE NOTES (Type of report and inclusive dates)

Final Report

5. AUTHOR(S) (First name, middle initial, last name)

A. W. Ruff

6. REPORT DATE

April 1974

7a. TOTAL NO. OF PAGES

30

7b. NO. OF REFS

14

8a. CONTRACT OR GRANT NO.

NAONR-31-73

b. PROJECT NO.

NBS 3120108

c.

d.

9a. ORIGINATOR'S REPORT NUMBER(S)

NBSIR 74-474

9b. OTHER REPORT NO(S) (Any other numbers that may be assigned this report)

10. DISTRIBUTION STATEMENT

Distribution of this document is unlimited.

11. SUPPLEMENTARY NOTES

12. SPONSORING MILITARY ACTIVITY

Department of the Navy
Office of Naval Research
Arlington, Va. 22217
Attn: Lt. R. Miller

13. ABSTRACT

The initial approach has been concerned primarily with the examination of particles recovered by the Ferrographic technique from samples of lubricating oils taken periodically during tests and service of bearings, gears, sliding surfaces, etc., in which such experimental variables as lubricants, lubricant additives, bearing materials, loads, etc., have been studied. Our examinations have been conducted principally using both Scanning and Transmission Electron Microscopy techniques, observing particle shapes, sizes, surface structures and other parameters as functions of distance along the Ferrogram and determining a semi-quantitative elemental chemical analysis of selected and typical particles. These electron microscope techniques have been used to characterize the wear particles and associated surface degradation produced in the bearing and gear tests conducted by others. They provide information on particles and surface details too small for study by optical microscopy methods.

DD FORM 1 NOV 65 1473 (PAGE 1)

S/N 0101-807-6801

Unclassified

Security Classification

14 KEY WORDS	LINK A ROLE	LINK A WT	LINK B ROLE	LINK B WT	LINK C ROLE	LINK C WT
Electron Microscopy						
Lubricated bearing systems						
Particle analyses						
Wear particles						

Table of Contents

	Page
Project Objective and Approach	1
1. Introduction	2
2. Experimental Details	3
3. Results and Discussion	4
3.1 Army Heavy-Lift Helicopter Gear Transmission	4
3.2 Ball Bearing Bench Test	4
3.3 Ball Bearing Bench Test	7
3.4 Single Ball Test	10
3.5 Bearing Ball Worn Surface	11
3.6 Bearing Ball Spalled Surface	12
4. Conclusions	12
5. Suggestions for Future Work	13
6. References	15

Objective

The objective of the program has been to characterize the wear particles and surface degradation produced by wear in bearing and gear tests in which the effects of several variables on failure of the wearing surfaces has been examined. The information obtained has been correlated with the results of allied studies conducted by others in an attempt to develop an understanding of the processes producing wear and degradation of metal surfaces in sliding, rubbing, rolling, and/or rotating contact and the effects of lubricants, lubricant additives, bearing materials, etc. on these processes. The characterization of the wear particles and wearing surfaces should aid in the establishment of the interrelationships between wear particle shape, size, size distribution, chemical compositions, metallurgical structure, and surface damage prior to failure.

Approach

The initial approach has been concerned primarily with the examination of particles recovered by the Ferrographic technique from samples of lubricating oils taken periodically during tests and service of bearings, gears, sliding surfaces, etc., in which such experimental variables as lubricants, lubricant additives, bearing materials, loads, etc., have been studied. Our examinations have been conducted principally using both Scanning and Transmission Electron Microscopy techniques, observing particle shapes, sizes, surface structures and other parameters as functions of distance along the Ferrogram and determining a semi-quantitative elemental chemical analysis of selected and typical particles. These electron microscope techniques have been used to characterize the wear particles and associated surface degradation produced in the bearing and gear tests conducted by others. They provide information on particles and surface details too small for study by optical microscopy methods.

After suitable techniques have been developed for examining and characterizing both the wear particles and the surfaces that produced them, these methods will be used to examine and evaluate specimens removed or obtained from programmed wear tests being conducted on associated programs.

1. Introduction

The study of wear debris particles recovered from the lubricating fluid in wearing contact systems has received increasing emphasis in recent years. Techniques for retrieving the wear particles, examining them, and monitoring the amount produced have been described.[1,2] Unusual particle morphologies have been reported and are proposed as possible indicators of particular wear modes.[3-5] Comparisons are being made between the results of spectrometric analysis of oil from wearing systems and measures of the amount of particulate debris in that oil.[2] Recently a wear theory has been proposed[6] that qualitatively predicts both the shape of the wear particle produced under specified conditions and the processes of plastic deformation and fracture that occur in the bulk material. Clearly much can be learned about the basic processes of wear and debris formation and about the prospects for monitoring wear in actual operating systems. Archard and Hirst[7] referred sometime ago to *mild* and to *severe* wear, distinguishing between a normal, slow degredative process and an abnormal, rapid destruction. The wear particle studies reported here include both contributions, and it is well to keep in mind that significance should be principally attached to observations of large, unusual wear particles.

This report concerns the examination and identification of particles found on Ferrograms of selected oil samples and the determination of suitable techniques for such identification. The Ferrograph instrument[1] enables particle collection from the lubricating oil on the basis of particle magnetic moment. It provides an initial selection of wear particles by rejection of nonmagnetic particles, thus saving analytical efforts. The resulting Ferrogram displays the wear particles collected into "strings" or groups oriented transversely to the oil flow direction as a result of transverse magnetic fields in the instrument. Deviations in this selection process occur when nonmagnetic particles adhere to magnetic particles in some manner and are thus collected. It is necessary to recognize that some types of particles important in the wear process, for example nonmagnetic abrasives, may not be collected reliably from the oil by this technique.

Particles having large magnetic moments are deposited first, near the entrance end of the oil on the Ferrogram. This leads to the development of a particle size gradient along the Ferrogram, larger particles depositing first. When a variety of types of material are present in the particulate collection, the sizing process is disturbed since large particles of a material with a relatively low specific magnetic moment will deposit further down the Ferrogram. For example, specific magnetic moment/unit volume values for three relevant materials in steel bearing systems are: Fe (171 m Tesla), Fe_3O_4 (48 mT), Fe_3C (99 mT). Thus physical sizing of particulates may scatter by at least factors of 4 or more along the Ferrogram as a result of material differences. As we shall see, examination of strings of particles in the Ferrogram does show a considerable size variation.

Initial results on this project have shown that considerable information can be developed from electron microscope studies of metal wear particles. Data on particle size, shape, composition, degree of oxidation,

contamination and deformation can be obtained using either scanning or transmission electron microscopy, electron diffraction, and X-ray emission analysis -- singly and in combination. Results of several specific studies will be presented.

2. Experimental Details

Various techniques have been developed to permit electron microscope evaluation of the particles on the Ferrograms. Initially, conventional glass Ferrogram slides were over-coated with vacuum-deposited carbon films (≈200A thick). That deposit provides sufficient electrical conductivity to prevent electric charge build-up during SEM study. Carbon is an excellent coating material in that no interference is presented for subsequent X-ray emission analysis of particulates. A second technique was developed that involved stripping the particles from the Ferrogram slide using a plastic replicating film and subsequently carbon-coating that film. The plastic film could then be dissolved in a solvent leaving the particle strings intact on a thin carbon substrate. That method has been used to prepare specimens for transmission electron microscope and diffraction studies on the particle strings.

A third method used glass slides that were previously coated with a thin vacuum deposited carbon layer. The oil sample was passed through the Ferrograph with the precoated slide in place. The particles were deposited on the slide in the usual manner. The carbon under-coating did affect the base-line optical density readings taken from the Ferrogram and in some cases contributed to oil overflow of the barrier strips along the sides of the Ferrogram slide. However, those problems do not appear serious. After usual washing procedures, the Ferrogram was heated in some cases for 30 seconds on a laboratory hot plate in air to remove residual oils and then examined directly in the SEM. While some charging of particles was seen in the SEM, it was found that sufficient electrical conductivity was present to permit detailed examination of the particles. Since no over-coating procedure was applied to these Ferrograms, all original surface features and details on the particles were preserved. Over-coating with another film (carbon or metal) was still possible if it was necessary for reasons of protection or fixation. Dislodgment of uncoated particles on these substrates during handling was noted and could be reduced by over-coating.

Examinations of solid bearing surfaces were conducted on a few components removed from service for various reasons. Further studies of this type are planned where the bearing surface wear conditions are carefully controlled.

Transmission electron microscopy and diffraction data were obtained using a 100kV electron beam with the specimen held in the conventional manner within a cryogenically-cooled enclosure to minimize specimen contamination. The limiting particle thickness for sufficient transmission would be about 0.25μm. The scanning electron microscopy data were obtained at 20kV beam potential with specimen currents in the range 0.1 to 10 nA and with the specimen held conventionally in a goniometer mounting. A Si(Li) X-ray detector system was available in the SEM with a FWHM of 170eV. The specimen was usually rotated to face the X-ray detector and specimen currents established at about 240 pA for X-ray analysis.

3. Results and Discussion

The results of examining wear particles obtained from a group of different lubricated systems will be described.

3.1 Army Heavy-Lift Helicopter Gear Transmission

The transmission from which this sample was taken had failed after a few hours of operation. There were many foreign or unusual particles detected on this Ferrogram that was produced at Trans-Sonics. The discussion will consider the classes of particles observed, originating at either gear or bearing surfaces. The entry deposit is shown in Fig. 1. The Ferrogram 2273 has been overcoated with a layer of vacuum-evaporated carbon. Some charging is seen at particles within the heavy, initial deposit. Many particles larger than 10μm are found near the entrance end of F-2273. Several small spheroidal particles were found (Fig. 1b). One of these is shown in Fig. 2a and contained only iron according to the X-ray emission analysis. A large faceted wear particle of unusual morphology is shown in Fig. 2b. Further down the Ferrogram the usual transverse strings of small wear particles are found, as shown in Fig. 3a. The character of these small ($\leq$ 1μm) rubbing wear particles is seen more clearly in Fig. 3b. A large foreign flake-like particle that is not ferromagnetic has settled there and subsequently the small wear particles were collected in strings that overlay it. The iron peak within the X-ray spectrum from the large flake is actually associated with these small wear particles that have originated from the gear surfaces.

The wear particle strings further down the Ferrogram are shown in Fig. 4 (rotated from the previous orientation). The variation in particle size within the strings is large. Many flake-like wear particles can be identified. In this field one iron spheroid is seen, as is another large foreign flake-like particle. Recently Cummins *et al.*[8] described observations on wear debris from a spur gear system. They reported principally small particles of thickness 0.2μm or less (note the small particle strings here in Figs. 3 and 4) together with some few spherical particles. The needle-like particles they observed were not found in the present sample. A large, faceted wear particle such as shown in Fig. 2b may originate in a fatigue-cracking process in the manner described by Venkatesh and Krishnamurty in their study[9] of cracking in gear systems.

These observations will now be compared with those made on wear particles obtained from lubricated bearing systems.

3.2 Ball Bearing Bench Test

The oil sample was obtained from SKF and originated from a lubricating system used during rolling bearing tests. The Ferrogram (F-2117) was prepared at Trans-Sonics using carbon precoated slides furnished by us. The same oil had been used previously to prepare F-1851 that was examined and will be discussed later. Optical examination of F-2117 at Trans-Sonics indicated the presence of cutting wear particles, spherical particles, and spalls. The entrance end of

the Ferrogram is shown in Fig. 5 at a relatively low-magnification (200x) scanning electron micrograph covering an area of about 0.5mm square. The remainder of the Ferrogram slide will not be discussed here but contained relatively few strings of small (< 1μm) particles. The study of F-1851 from this same oil concentrated on smaller particle strings and will be discussed later. Figure 5 shows that some larger particles do not have sufficient conductivity to the carbon-undercoated glass slide and acquire an electrical charge during a slow beam scan, causing streaks on the photographs. This was rarely noted and caused no significant problem. The labeled areas in Fig. 5 are examined at greater resolution in the following photographs.

The region A is shown at higher magnification in Fig. 6. Many flake-like particles are seen, the larger ones being about 10μm in lateral dimensions and of the order of 0.1μm thick. Most of the flakes are bent and corrugated with ragged edges and evident surface features such as lines or bands. Many small particles, less than 1μm in size are also seen. The larger flakes presumably fractured or spalled away from the bearing material during contact wear and stressing. They could subsequently have been further deformed if recirculated through the bearing contact regions by the lubricating oil and even fractured again to produce some of the smaller particles. The expected EHD film thickness would be one-tenth or less the size of these particles (order of 10μ-inch = 0.3μm).

It is of interest to estimate the numbers of particles collected in these strings. Cursory inspection of Fig. 6a indicates about 10^2 particles in the field, ignoring particles below 0.5μm size. Examination of other subfields of Fig. 5 indicates that to within factors of 3, the total particle count in Fig. 5 can be estimated at about 3×10^3 particles. This number should be kept in mind in connection with the validity of conclusions drawn from individual particle analysis and extended to the macro-system. One clear drawback of the Ferrogram technique for microscopic evaluation is seen in Fig. 6. It involves the tendency for particles to clump and overlay one another in the strings. This prevents accurate particle counts and particle sizing and may affect other observations, in particular X-ray emission analyses. However, dilution and redispersion techniques should be applicable where the particle densities are too large.

Another region from Fig. 5 is shown in Fig. 7. One observes substantial differences in contrast between the particles. The particles showing lower secondary electron emission (grey images) are probably more heavily oxidized and hence contain less iron. Some particles show a porous surface structure that is also suggestive of oxide material. It is recalled that the particles have not been overcoated prior to examination, hence the existing surface structures are preserved. Flake-like particles are observed together with several rod-like particles.

The region E from Fig. 5 is shown in greater detail in Fig. 8. One flake-like particle in this string has considerable surface structure that includes several cracks and smaller, attached particles. A spheroidal particle (2.4μm diameter) is also seen. Its size is sufficiently large to contain nearly all the X-ray emitting volume permitting meaningful X-ray emission analysis. However, fluorescence effects associated with neighboring particles in such a collection could be substantial and require correction. Analysis of this spheroid showed only an iron peak in the X-ray emission spectra as shown. The large flake-like particle contains a significant amount of iron and zinc.

Results of X-ray emission analyses on other particles are shown in Fig. 9 taken from region F in Fig. 5. Two particle analyses are shown, one from another spheroid about 2.5μm in diameter and the other from an irregularly shaped 3μm particle. The background analysis was obtained from area c. Analysis was conducted using a stationary electron probe, an electron beam potential of 20kV, a beam current of 200pA, and a counting time of about 100 seconds. Both particles are iron with no other elements present.
The background contains elemental emissions from oil residue material on the substrate, principally Si, K, Ti and Zn (some of the Si peak originates in the glass substrate).

It is important to recognize the limitations present in X-ray emission analysis conducted on particles of widely different size, shape and composition, collected into close physical contact. Beaman and Isasi[10] indicate many of the general considerations including the use of energy-dispersive detection systems. Even where only qualitative or semi-quantitative information is desired, great care must be taken to avoid adjacent particle interferences by X-ray flourescence, absorption, and emission due to back-scattered electrons. Point-probe analysis must avoid exciting small surface contaminant particles on larger particles. Penetration through the particle of interest into other particles below must be recognized when present. This study generally has examined reasonably well isolated particles larger than 2μm in size and oriented favorably with respect to the X-ray detector. Bayard[11] has determined the relation between particle (spherical) size and X-ray intensity (relative to bulk) for aluminum particles. We have estimated using his results and data on the X-ray distribution in depth for copper and aluminum[10] that Fe particles of diameter 0.5μm should yield an X-ray intensity about 75% that of bulk. At a diameter of 1.5μm, the intensity should exceed 95% of the bulk value. Techniques for true quantitative analysis of small particles are described by Bayard[11] and are under further development in several laboratories.

The region (G) in Fig. 5 is shown in more detail in Fig. 10. A small string of seven particles is present containing a spheroid of 4.5μm diameter. One of the particles has a chip-like appearance and another (c) shows significantly lower image contrast. The X-ray spectra from particles a, b, c and background d are shown in Fig. 10(c). The spheroid and particle b are iron, however, particle c shows a weak

iron line and a significant Si, K, and Zn content. Since these three elements are associated with oil residue, it appears that particle c may be iron oxide that has absorbed a significant amount of oil.

Another string of particles from this sample is shown in Fig. 11 together with the particle X-ray analyses. The faceted spheroid (a) is a chromium-containing iron as is particle (e). Particles (b) and (f) contain principally iron. Particles (c) and (d) are iron oxide particles containing significant oil residue as indicated by the Si and K peaks. These results are summarized in Fig. 12 where the various X-ray peak heights are given. Note the variation in electron emission among the particles seen in Fig. 12 in the Y-modulation image (where emission is proportional to Y-deflection of the signal trace).

In summary, the bearing test oil sample contains a wide distribution of particle sizes and types, some results from which are summarized in Table I. Many examples of flake-like particles are found (perhaps about 25% of the total in the size range 1 to 10μm. Some elongated, rod-like particles are found. Four spheroidal particles were found (from an estimated total of 3×10^3). Three of those (size 2.4μm, 2.5μm, and 4.5μm) were analyzed by X-ray emission and found to contain only iron. Contrast differences were found among the particles imaged by secondary electron emission. They are believed associated in some cases with the iron/iron oxide ratio of the particles.

3.3 Ball Bearing Bench Test

A second study was conducted on wear particles from the SKF test of 52100 steel ball bearings. Rather than carbon-coat the Ferrogram-1851, we removed the particle strings from the glass substrate by extraction replica techniques. This would permit high resolution imaging in a transmission electron microscope (TEM) and transmission electron diffraction (TED) examination, particularly of the smaller particles. A softened polymer film was pressed onto the Ferrogram, allowed to harden, stripped off, and overcoated with carbon, and then the polymer film was dissolved in solvent. The resulting carbon film contained the partially embedded particle strings and was supported on a conventional copper grid that could be loaded directly into the TEM specimen holder. Figure 13a shows two strings located in one grid opening. This same area is shown in the optical microscope photograph in Fig. 13b, indicating the versatility in this preparation and mounting technique.

Two specific strings of particles will be discussed among several that have been examined from F-1851. String S_1 is shown in more detail in the SEM photograph of Fig. 14. The particle size varies from about 0.1 to 2μm; other strings contained larger particles. The difference in emissive-mode contrast between particles is evident. Some particles appear thin and flake-like, others are more equiaxial. Some angular features are seen on certain particles. Data on Fe-Kα X-ray emission have been obtained on the particles labeled A, B, and C; particle C contains significantly less iron.

TABLE I.

SELECTED PARTICLE CHARACTERISTICS FROM F-2117:
LUBRICANT FROM ROLLING BEARING TESTS

Particle			Peak Heights (K_α - 1,000 cts)
Shape	Size (μm)	Identification	Fe : Other
spheroid	3	alloy steel	11 : 2.7Cr
spheroid	2.4	iron	10
spheroid	2.5	iron	12
spheroid	4.5	iron	10
lump	3	iron	11
lump	3	iron oxide	6.8 : 5.2Si
lump	2	alloy steel oxide	4.8 : 2.3Cr : 2.6Si
lump	1.5	iron	8.4
lump	3	iron	12
lump	4	iron	11
lump	3	iron oxide	3.2 : 8.4Si
flake	3	iron oxide	3.2 : 7.4Si
flake	8	iron/zinc	2.6 : 3.6Zn
flake	10	iron	11
flake	10	iron	11
flake	2	iron	12
free spheroid	2.5	foreign	1.3 : 7.8Si : 4.5Al

Transmission electron micrographs of string S_1 obtained at 100kV accelerating potentials are shown in Fig. 15. Here satisfactory penetration is obtained at thicknesses of 2000Å or less for iron particles. Thicker particles will appear black, only the outline regions being thin enough for penetration. The labeled particles have been studied by electron diffraction. Particles C, D, E, and H have a strong iron oxide diffraction pattern together with an α-iron diffraction pattern. These particles are 50% or more composed of a mixture of two oxides, Fe_2O_3 and Fe_3O_4, the balance being iron. Particle A has a lower but still significant iron oxide content; it is relatively thin and flake-like. Particles B, F, and G are thick (greater than 0.5μm), composed of iron with a covering of the combined oxide mentioned above. Further information on particles A and B is shown in Fig. 16. Two dark field images are shown using different reflections, along with the bright field image and the diffraction pattern from particle A. In dark field imaging only crystalline regions oriented precisely for diffraction into a narrow angular region will appear bright or in contrast. Examination of the images shown indicates that particle A is composed of many small (200-500Å) crystal regions of both iron and iron oxide. It has the structure expected from a deformed iron fragment that had recrystallized and partially oxidixed. The remaining (residual) strain level is not high, as evidenced by the diffraction pattern. Particle B offers less information due to its thickness, however, its surface appears covered with an oxide film or collection of oxide particles. The fine structure in the dark field images suggest the latter covering is more likely.

In summary, the string S_1 contains a number of different particle types. Thinner particles may be solid iron, composed of many crystallites (A), they may be a loose collection of much smaller iron oxide particles (C), or they may be relatively thick iron particles with an oxide coating (B). No carbide particles were found in this string. A more detailed electron diffraction pattern is shown in Fig. 17 with the principal lines for α-Fe and Fe_3O_4 identified. The Fe_2O_3 pattern contains two additional lines that serve to distinguish it. As long as sufficient diffraction intensity is obtained, solutions of patterns from particles are straightforward.

Another string (S_2) is shown in Fig. 18. Again considerable size and shape variation among the particles is seen. Fine structural details can be observed here in emissive mode imaging. The brightness differences between particles are seen again in this string. A portion of this string is shown in the TEM micrograph composite of Fig. 19. The labeled particles have been studied in diffraction. Particles 1, 3a, 3b, 9b, and 12 give principally iron oxide patterns. Particles 2, 4, 5, 7, 10, 13, 14, and 15 give strong α-Fe patterns. The remaining particles studied showed both iron and iron oxide content to a substantial amount. Some of the thinner particles (10, 13, 14, 15) appear to be solid, partially-oxidized iron fragments. Other particles (3a, 9a) appear to be more a collection of small fragments, principally iron oxide.

These observations are rather similar to those made on string S_1 and suggest that a sufficiently valid description of the (smaller) wear particles on F-1851 can be made on the basis discussed. Over seventy electron diffraction patterns have been analyzed. About one-half are mixtures of α-Fe and iron oxide, about one-quarter are predominantly iron, and the remainder are principally iron oxide particles. No carbides have been found. Some foreign crystallites outside of the particle strings have been identified. The vast majority of particles in string groups in this Ferrogram are iron fragments, partially or completely oxidized. The low incidence of foreign particles within the strings illustrates the advantage of the Ferrograph particle selection and display technique in studying wear particles.

In a study of wear of cast iron in dry sliding, Takeuchi[12] reported a variation in iron oxide amount detected by diffraction measurements, dependent on sliding distance and presumably surface temperature. For long accumulated wear distances, the wear debris was predominantly iron oxide. Those observations are consistent with the variation in amount of particle oxidation seen here. The absence of carbide particles in the wear particle strings examined was surprising in view of the known importance of carbide content in steels on their wear behavior (see, for example, Hurricks[13]). However, particles smaller than 0.5μm have not been systematically studied here by electron diffraction. Carbides dislodged from the steel bearing surfaces may fracture into rather small particles and thus escape detection. Brief X-ray diffraction examination of a few wear debris samples has also not indicated significant carbide content.

3.4 Single Ball Test

A series of oil samples from a test of an M50 steel (includes 4% Cr, 4% V) ball and race was obtained by Trans-Sonics and processed to produce several Ferrograms. A silicon-bronze ball retainer was included in the mechanical testing device. The oil was MIL-L-23699 type held at a temperature of 300°F. The test involved a time-to-failure of 9h 55m and a ball Hertz stress of 600 kpsi maximum. At failure the ball became driven into the retainer. The Ferrogram (F-2119) was prepared using carbon precoated slides from an oil sample taken at 8h time (1h 55m prior to failure).

A low magnification view of the entrance end of this Ferrogram is shown in Fig. 20 covering an area about 0.9 by 2.7mm. Three large particle strings are seen and will be examined in more detail. The remaining areas of the Ferrogram contained isolated particles or small particle (< 1μm) strings and have not been examined closely. The particles are in place on the precoated-carbon Ferrogram slide and have not been overcoated.

Region A in Fig. 20 is shown again in Fig. 21. Several examples of long ribbon-like particles are found in that string together with some flake-like particles. Both types have surface structures and markings that suggest plastic deformation and slip bands. X-ray analysis results are given. Figure 21 shows the region B in more detail. One

curled ribbon particle is seen in this string. Several small particle strings are present in this area but also in the area of region A. Comparison of Figs. 21a with 22a and Figs. 21b with 22b shows the particle sizing capability of the Ferrograph instrument. The larger particles predominate in region A, however, many smaller particles (1 to 4μm) appear present in both regions. Those regions are separated by 0.45mm along the Ferrogram. It seems that the larger magnetic moment particles are deposited earlier on the Ferrogram but that smaller moment particles may deposit either (i) adjacent to larger particles (within their strings) near the entrance end or (ii) further down the Ferrogram in strings of like-sized particles. That "early deposition" behavior may result from relatively large magnetic field gradients within the incomplete, forming particle strings.

The final region (c) studied in Fig. 20 is shown in detail in Fig. 23. The larger flake-like particles are clearly present in this region as is one large, 8μm diameter spheroid. The spheroid is remarkably smooth and free of surface structures as compared to adjacent particles. X-ray emission spectra from four of the particles are shown in Fig. 24. Particle c produces a single iron peak, however, the spheroid produces a weak iron peak together with strong silicon and aluminum peaks. None of the other particles analyzed showed these Si and Al peaks. The flake-like particle d contains significant amounts of Cr and Ni, an alloy steel. The globular particle e also contains Cr and Ni together with a significant amount of copper, presumably resulting from the silicon-bronze retainer. X-ray signal imaging studies were conducted on this string using the prominent Fe K_α and Si K_α lines. Those X-ray scans proved the low-iron, high-silicon content of this particular spheroid which may have originated as a nonmetallic inclusion in the steel ball or race.

In summary, only one spheroid has been found among the particles from this single ball test. It is relatively large and it contains significant amounts of silicon and aluminum. There is no appearance of a rough or cracked oxide covering on the sphere. Adjacent particles in the string that show a greater roughness do not show any significant silicon content. The ribbon-like particles found in this Ferrogram are typical cutting-wear particles.

3.5 Bearing Ball Worn Surface

A disassembled bearing that had failed during a bench test at SKF was examined to attempt to relate the particle debris obtained by the Ferrograph from the lubricating oil with the bearing surface structures and markings. An example is shown in Fig. 25 taken from one 52100 steel bearing ball. Some of the surface tracks seen in Fig. 25a may remain from initial finishing operations, however, many examples of deep wear gouges are present. Detailed examination indicated that plastically deformed metal at the gouge rim can be detached in the form of small particles (Fig. 25b). Larger particles may also form in this way as indicated by the 3μm particle formed in Fig. 26. Note the surface markings on the particle and the similarity with the bulk surface markings. This particular gouge appears to be

abrasively formed and the particle is formed from the edge displaced metal. The degree of plasticity of the surface material is apparent. Endo and Kotani[14] have recently reported similar topographic observations on steel surfaces wearing under lubricated sliding conditions.

3.6 Bearing Ball Spalled Surface

This ball was obtained from a failed bearing supplied by the Naval Ships Engineering Center and previously studied at Trans-Sonics. A spall occurred on the ball surface whose appearance (Fig. 27a) is typical of that type of damage. Considerable subsurface cracking is seen in this example extending away from the exposed fracture surface. The fracture surface morphology suggests that some plastic behavior occurred, perhaps after the spall fragment was produced. Many leaf-like protrusions remain on the surface, perhaps as a source of additional wear particles during subsequent contacts and motion. Several spheroidal particles were located on this surface, and a stereo-pair of SEM photographs of them is shown in Fig. 28. These spheres are not solid, metallic particles, however, since the X-ray emission peak intensity is considerably less than that obtained from the background and from other particles on the surface. They appear to be composed of iron and organic constituents.

4. Conclusions

Several different approaches to the study of metal wear particles using microscopy and diffraction techniques have been evaluated and illustrated in this report. The principal findings are as follows:

(1) The Ferrograph technique can reliably extract ferromagnetic wear particles from a lubricating oil sample and deposit the particles on a substrate suitable for microscopic examination.

(2) The particles are deposited so that smaller, lower magnetic moment particles are located further from the entrance end of the Ferrogram. The physical sizes of the particles may deviate by a factor of 5 within one particle string, due to local magnetic field gradients.

(3) Nonmagnetic particles are found randomly deposited on the Ferrogram, generally not within the strings of magnetic particles. However, examples have been found of particles containing a small proportional amount of iron located in such strings. The iron content may be transferred wear metal in some cases.

(4) The glass substrate Ferrogram can be examined in the SEM after overcoating with about 200Å of carbon. Carbon precoated glass slides can be used in the Ferrograph and examined without overcoating. This preserves any original particle surface features. Care must be taken with such preparations or particles may be dislodged during handling. Plastic film extraction type replicas can be taken from the Ferrograms in order to examine the particles in transmission microscopes.

(5) The particle density within the strings is too large for certain analyses. Particle sizing and shape classifying would not be possible. X-ray emission analysis is complicated by excitation or absorption in neighboring particles. Techniques for recovering particles from a Ferrogram of interest, after dilution and redeposition of the particles on suitable substrates can probably be developed.

(6) X-ray emission analysis of individual particles by electron beam excitation can be conducted. Iron particles as small as 2μm in diameter can be studied. Many precautions are noted that must be considered in such studies. Semi-quantitative analysis requires corrections for substrate and neighboring particle effects.

(7) Considerable differences are noted in the intensity of the emissive mode images of wear particles in the strings. These differences are due to particle composition, density, and thickness. The differences can be used in some cases to identify the particles.

(8) Transmission electron diffraction studies have revealed differences in the amount of oxidation of iron wear particles, presumably related to different histories of the particles. Carbide particles have not been detected but may be present in the size range $\leq$0.1μm that has not been carefully examined.

(9) Spheroidal particles have been observed in nearly all oil samples examined, including both gear wear and bearing wear samples. Typically from one to five spheroids may be found on one Ferrogram, i.e., a very small proportion of all wear particles. The surfaces of those particles are relatively smooth in nearly all cases. X-ray analysis has proven that the small (<5μm) spheroids usually produce only an iron emission line. Larger spheroids have been identified as having significant concentrations of other elements and may be oxides, silicates, etc. Some of the larger (>5μm) spheroids may be partially composed of organic materials.

(10) Comparison of gear wear with bearing wear particle collections indicates that significant size differences exist in the particle distributions. Gear wear particles are generally smaller. Quantitative information on the particle size and shape distributions is required.

(11) Examination of worn bearing surfaces indicates that displaced material involved in the process of wear particle formation can be detected. The SEM reveals a surface morphology that suggests considerable plastic deformation near the surface. Signal processing conditions that produce a maximum contrast level are essential in examining surface morphologies using the SEM.

5. Suggestions for Future Work

It is necessary to characterize the bulk surfaces from which wear particles originate. The bulk phases present and their size and structure should correlate with the particle characteristics observed. Shape and size classification of the wear particles should be undertaken using automated

image analysis techniques. It does not appear possible to conduct sizing, counting, and shape classifying operations on the particles in the present Ferrograms due to problems of clustering and overlap. However, redispersion and dilution of the particles on a substrate should be possible. Unusual particle morphologies must be examined carefully, including spherical and cutting-wear particle shapes. Residual stress studies on the particles can be conducted using techniques of electron channeling and electron transmission.

Acknowledgments

Much of the work reported here could not have been accomplished without the cooperation of V. C. Westcott, R. W. Wright, and J. L. Middleton of Trans-Sonics, Inc. and Dr. H. Dalal of SKF Industries, Inc. The advice and support of Lt. R. Miller, ONR, and P. Senholzi, NAEC, is gratefully acknowledged. The author also appreciates the assistance of several colleagues at NBS, particularly the efforts of Dr. Anna Fraker during a phase of the TEM study.

References

1. W. W. Seifert and V. C. Westcott, "A Method for the Study of Wear Particles in Lubricating Oil," Wear 21, 27 (1972).

2. V. C. Westcott and W. W. Seifert, "Investigation of Iron Content of Lubricating Oil Using a Ferrograph and an Emission Spectrometer," Wear 23, 239 (1973).

3. D. Scott and G. H. Mills, "A Scanning Electron Microscope Study of Fracture Phenomena Associated with Rolling Contact Surface Fatigue Failure," Wear 16, 234 (1970).

4. E. Broszeit and F. J. Hess, "Discussion to 'A Scanning Electron Microscope Study of Fracture Phenomena Associated with Rolling Contact Surface Fatigue Failure,'" Wear 17, 314 (1971).

5. D. Scott and G. H. Mills, "Spherical Debris - Its Occurrence, Formation and Significance in Rolling Contact Fatigue," Wear 24, 235 (1973).

6. Nam P. Suh, "The Delamination Theory of Wear," Wear 25, 111 (1973).

7. J. F. Archard and W. Hirst, "The Wear of Metals Under Unlubricated Conditions," Proc. Roy. Soc. A236, 397 (1956).

8. R. A. Cummins, E. D. Doyle and B. Rebecchi, "Wear Damage to Spur Gears," Wear 27, 115 (1974).

9. V. C. Venkatesh and R. Krishnamurty, "Intergranular Cracking During Pitting of Gears," Wear 25, 329 (1973).

10. D. R. Beaman and J. A. Isasi, "Electron Beam Microanalysis," ASTM publication STP 506 (1972).

11. M. Bayard in Microprobe Analysis, ed. C. A. Andersen (J. Wiley and Sons, N. Y., 1973) p. 323.

12. E. Takeuchi, "The Mechanism of Wear of Spheroidal Graphite Cast Iron in Dry Sliding," Wear 19, 267 (1972).

13. P. L. Hurricks, "Some Metallurgical Factors Controlling the Adhesive and Abrasive Wear Resistance of Steels. A Review," Wear 26, 285 (1973).

14. K. Endo and S. Kotani, "Observations of Steel Surfaces Under Lubricated Wear," Wear 26, 239 (1973).

Fig. 1(a). Ferrogram F-2273, oil sample from helicopter gear transmission box. Oil flow is downward. Initial particle deposit region is shown. M = 100x.

(b). Region near A above. Several spheroidal particles are seen (arrows). M = 500x.

Fig. 2(a). Spheroidal particle shown above. X-ray spectrum indicated only iron in spheroid. M = 2,000x.

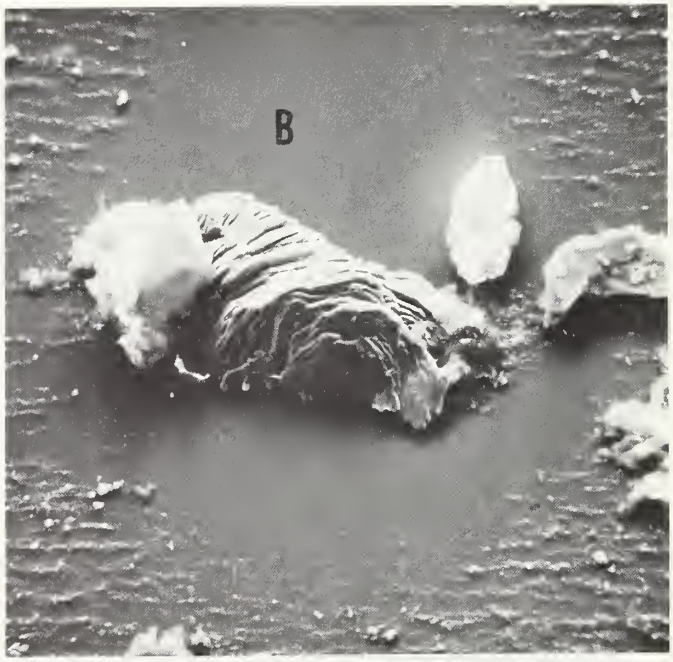

(b). Region B near initial deposit showing large faceted, iron wear particle. M = 500x.

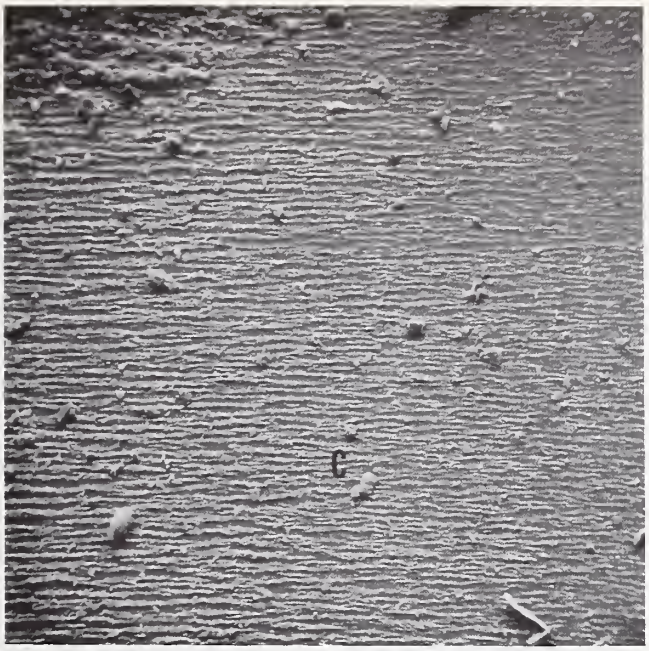

Fig. 3(a). F-2273 region just below initial deposit. Oil flow is downward. Note characteristic transverse strings of small wear particles. M = 100x.

(b). Region C showing large flake underneath small wear particle strings. X-ray spectrum from upper portion of flake is shown. M = 1,000x.

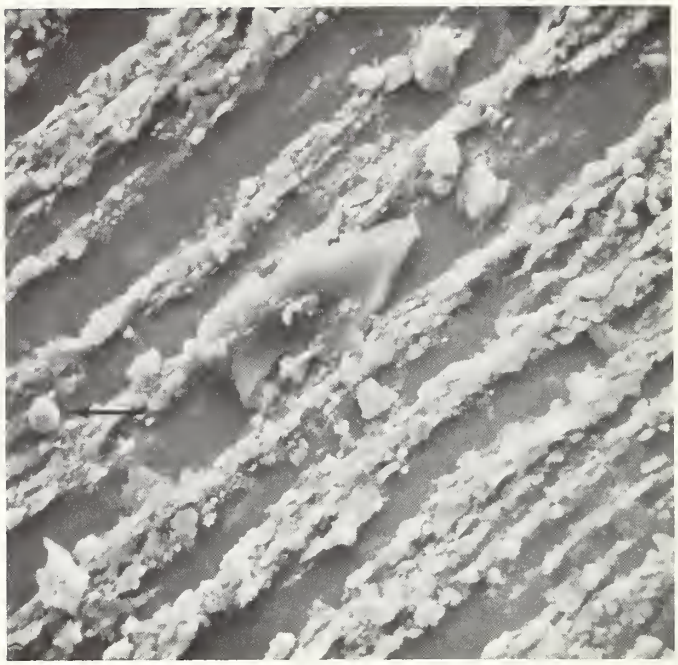

Fig. 4. Region further down from initial deposit in F-2273. Note spheroid at arrow. Particle size in strings varies from 5μm to well below 1μm. Many flake-like particles are found. M = 1,000x.

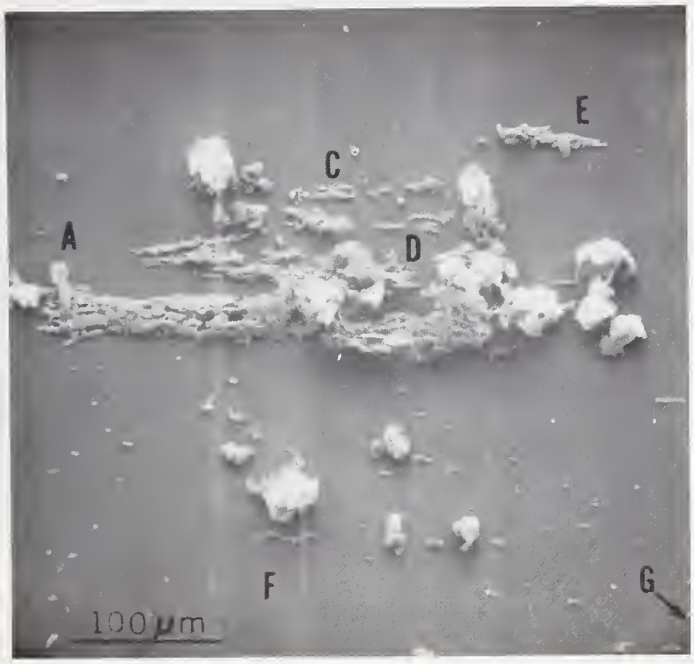

Fig. 5. Ferrogram #2117 from SKF service tank oil, lubricating bearing tests. Carbon-undercoated Ferrogram, scanning electron micrograph, M = 200X. Region shown is at entrance end, oil flow downward. Some particles (metal?) are charging in electron beam due to insufficient electrical contact with substrate. Regions labeled are shown in several subsequent photographs for greater detail on particles.

Fig. 6(a).Region A from above. Many flake-like particles are seen in size range 1 to 10 μm. M = 1,000X.

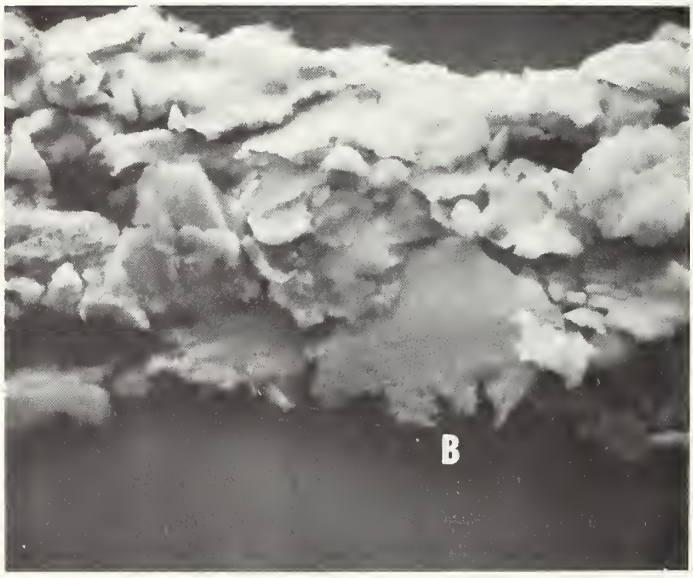

(b). Region near B from above. Surface structures on particles near B appear as slip or deformation lines. Flake above B and flake at left contain only iron. M = 2,000X.

Fig. 7(a). Region D from above. Several small particles strings are shown together with some isolated particles. M = 1,000X.

(b). One string from above area containing particles showing different emissive image contrast as previously reported. M = 4,000X.

Fig. 8(a). Particle string from Region E in above. Many flake-like particles are seen with resolvable surface structures. M = 1,000X.

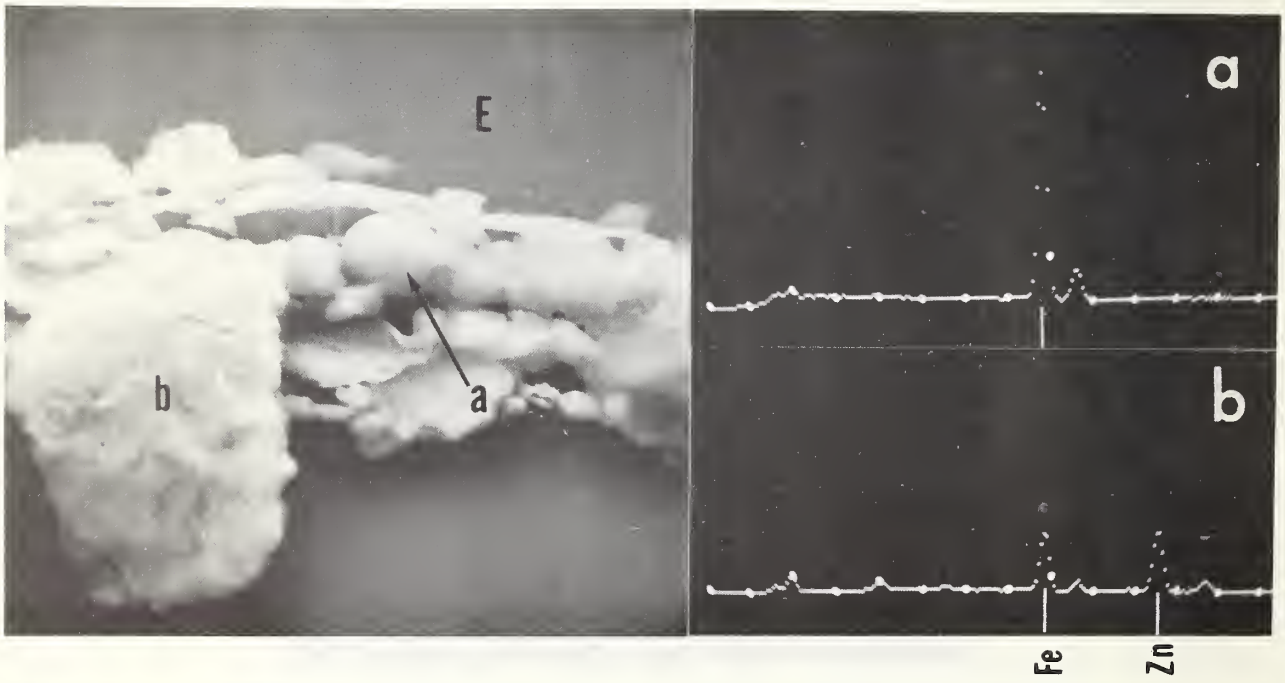

(b). Details in above particle string. Note surface features on large flake at left. Spheroidal particle (a) of 2.4 μm diameter is shown. X-ray analysis indicates (a) spheroid contains only iron and (b) flake has reduced iron and significant zinc content. M = 5,000X.

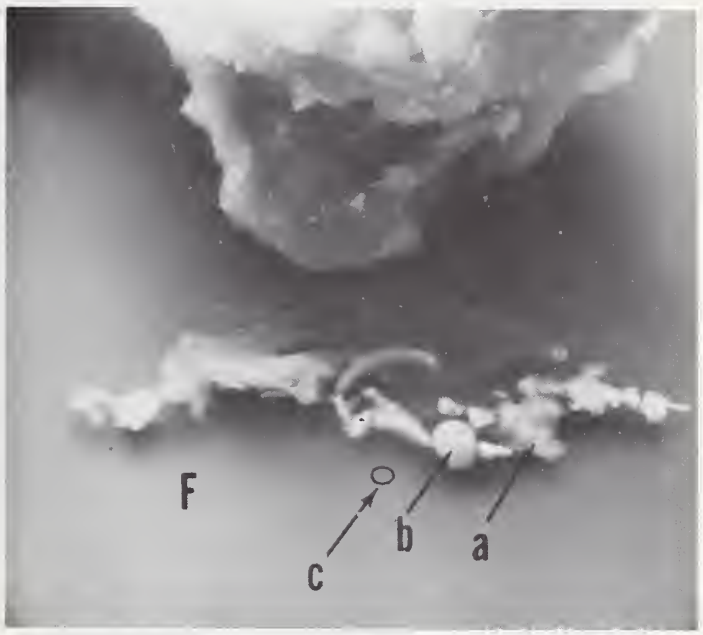

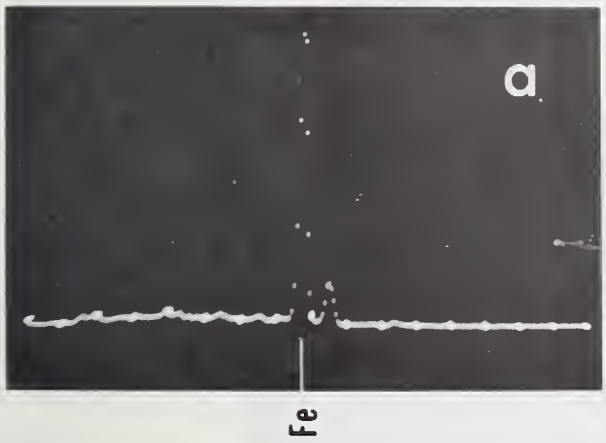

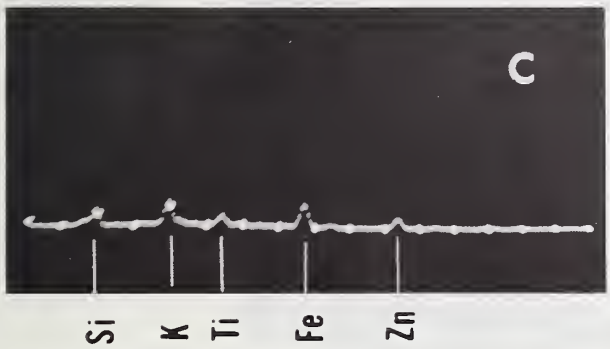

Fig. 9. Region F from above. String contains several particles, one of spheroidal shape (b) of 2.5 μm diameter. X-ray emission spectra are shown for particles (a) and (b) and background region (c). Both particles are iron. M = 2,000X.

Fig. 10(a). Particle string from Region G in Fig. 5. (slightly outside area shown). Spheroidal particle diameter is 4.5 μm. Large blob gives typical background X-ray spectrum. M = 1,000X.

(b). Details of above string. Note contrast differences between particles. X-ray emission spectra were obtained from labeled particles. Spheroidal particle is iron. Particle (c) contains oil residue. M = 2,000X.

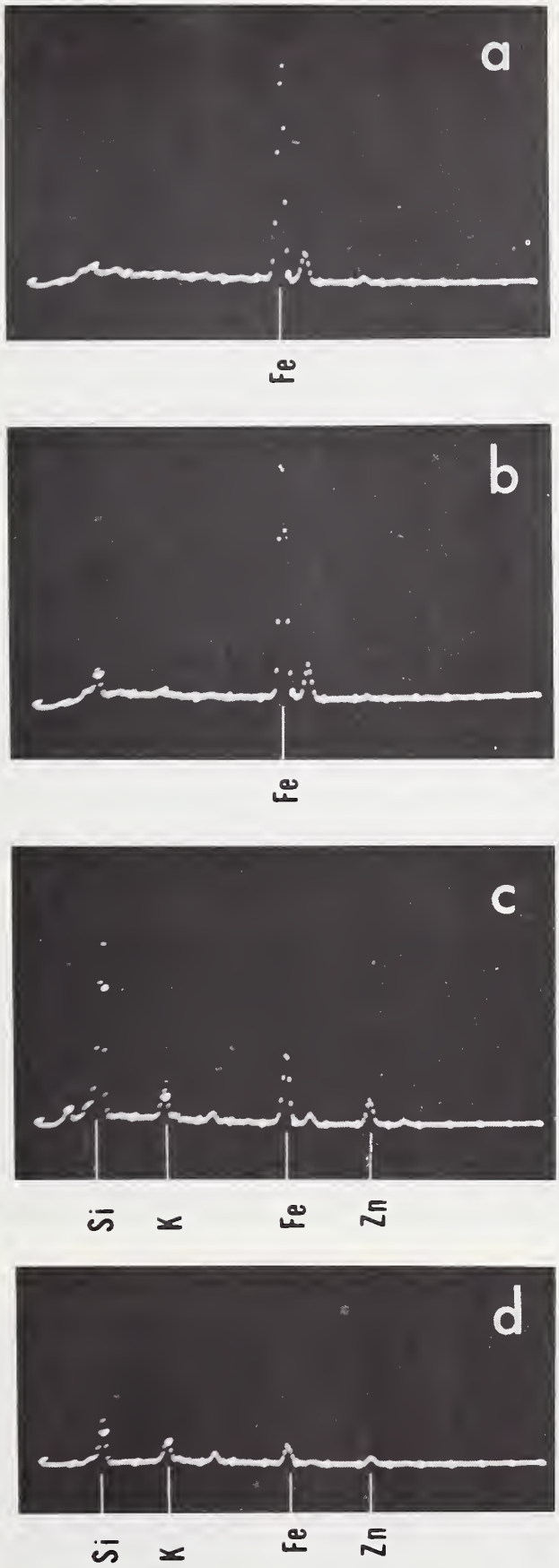

10(c). X-ray spectra from particles (a), (b), (c), and background (d).

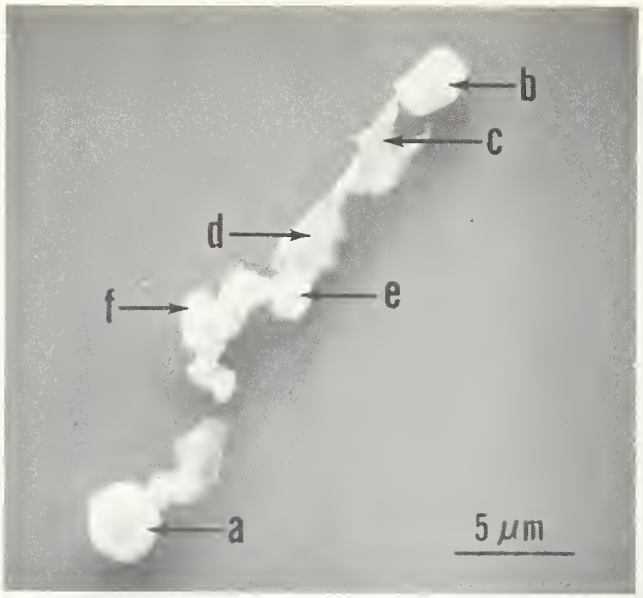

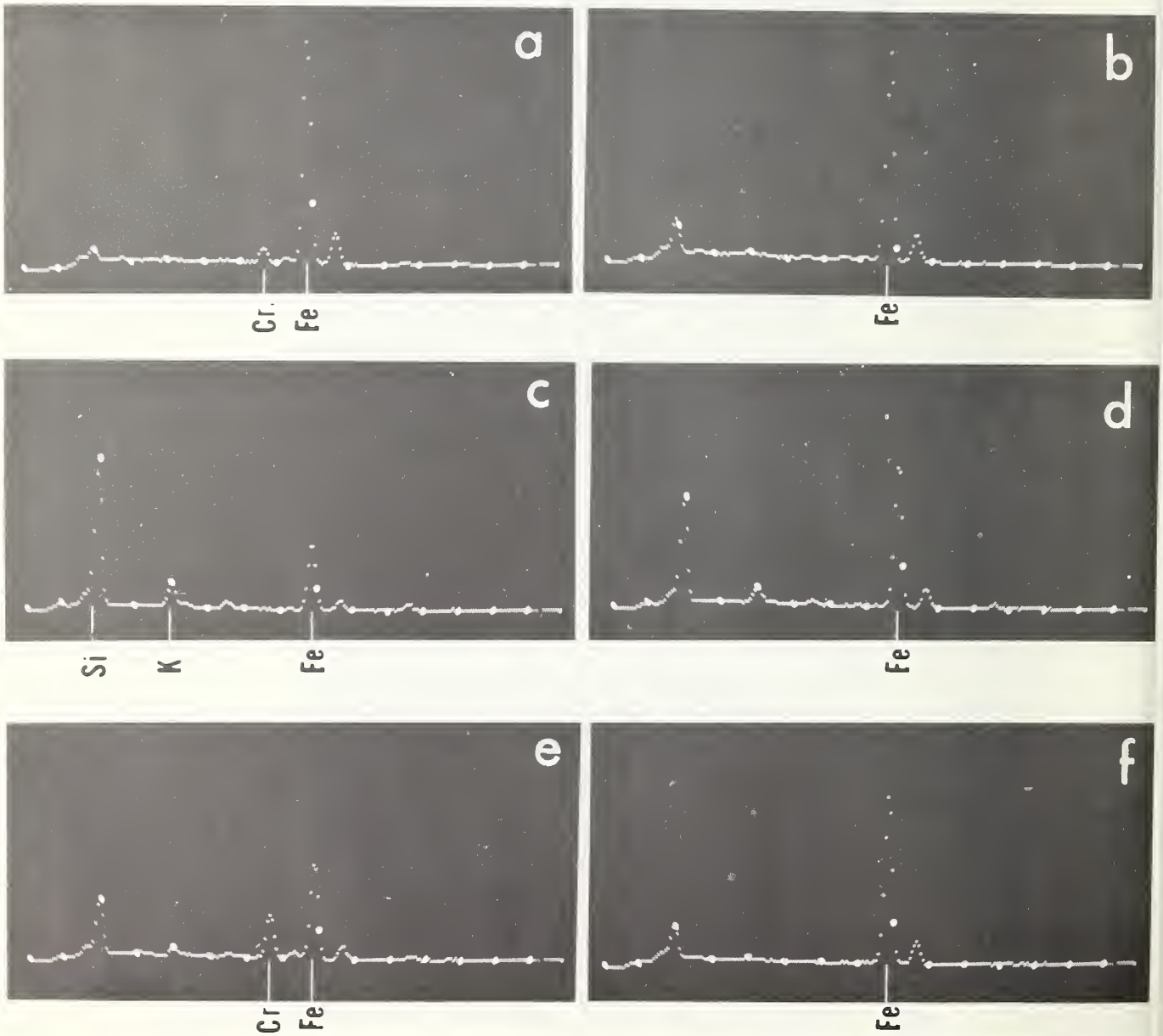

Fig. 11. Particle string from F-2117 with X-ray spectra as indicated.

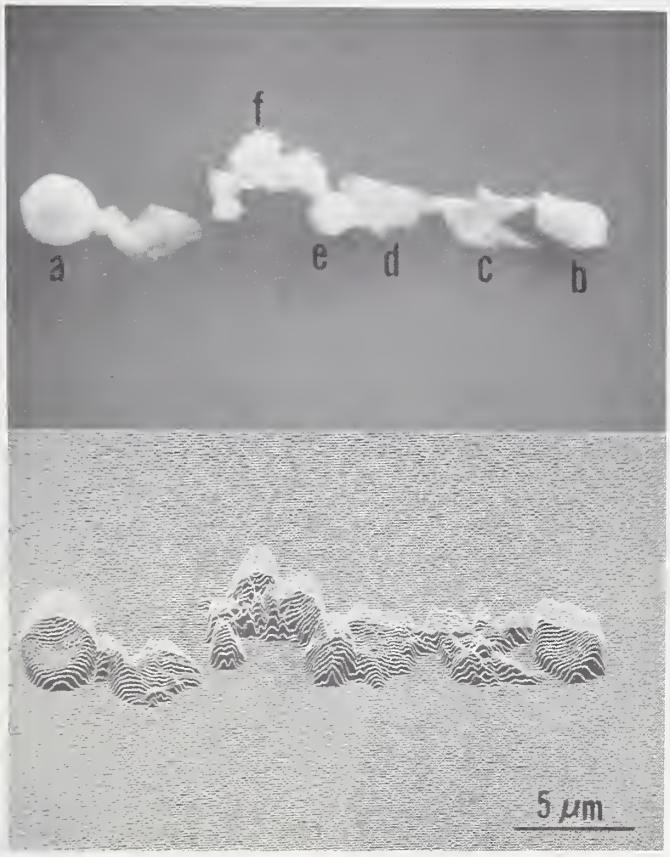

Particle			Peak Heights K_α - 1,000 cts Fe : Other
Shape	Size (μm)	Ident.	
a - spheroid	3	alloy steel	1.1 : 0.1Cr
b - lump	3	iron	1.1
c - flake	3	iron oxide	0.3 : 0.7Si
d - lump	3	iron oxide	0.7 : 0.5Si
e - lump	2	alloy steel oxide	0.5 : 0.2Cr : 0.2Si
f - lump	1.5	iron	0.8

Fig. 12. Particle string above showing intensity variations in Y-modulation. Analysis results are shown.

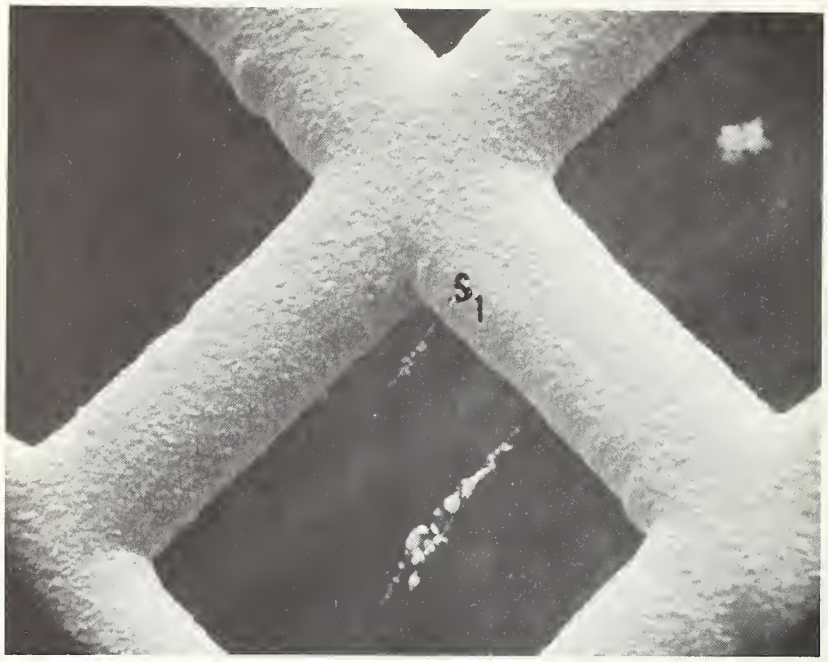

Fig. 13(a).
F-1851. One support grid opening containing two particle strings on carbon film in SEM. M = 600x.

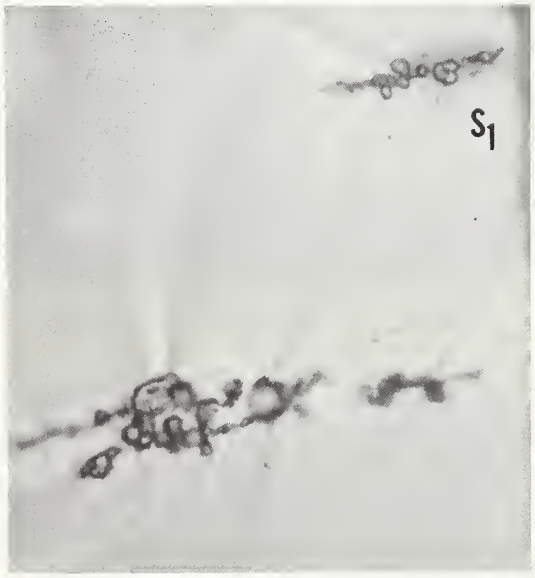

(b). String S_1 on carbon replica in the optical microscope. M = 1,000x.

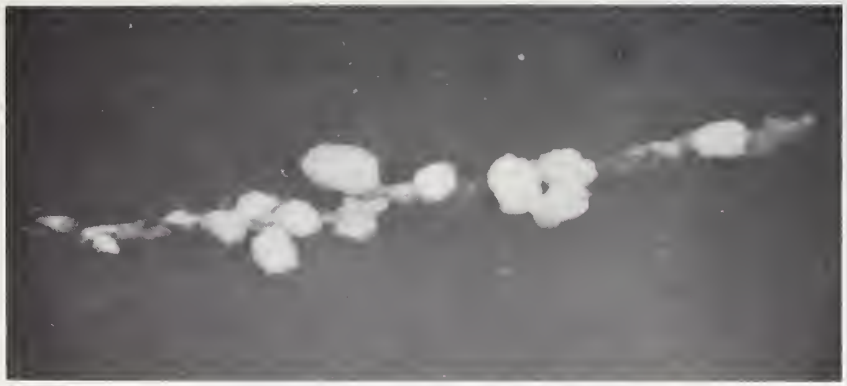

Fig. 14.
F-1851. String S_1 in SEM. Note contrast differences among particles. M = 5,500x. Details below at M = 11,000x.

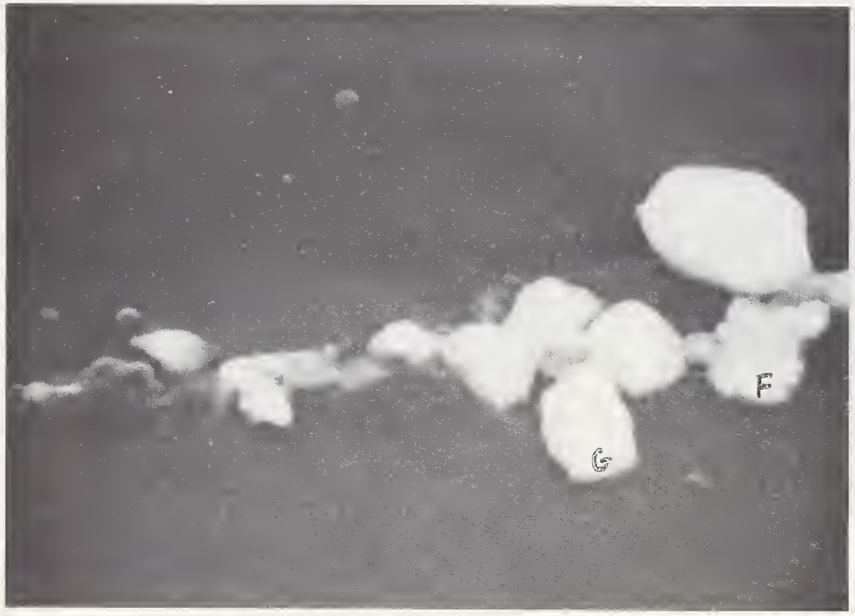

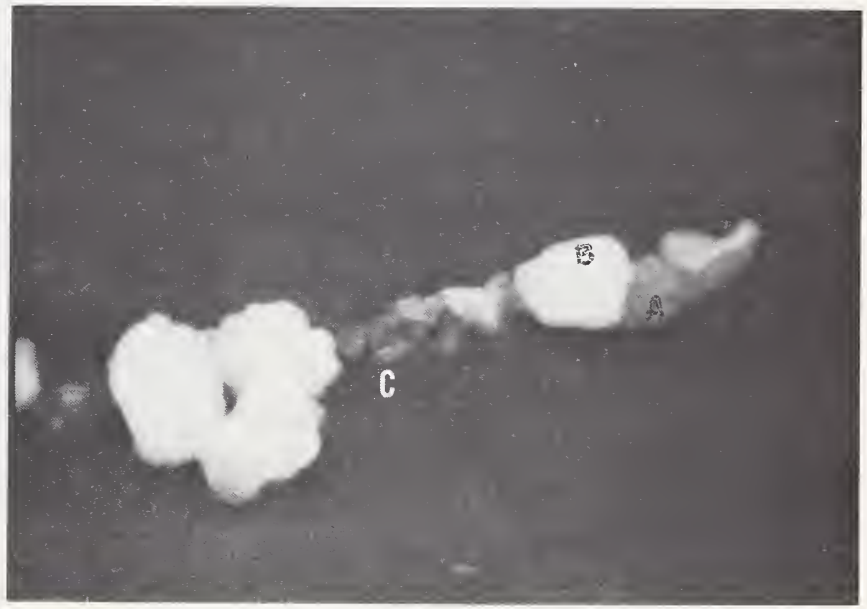

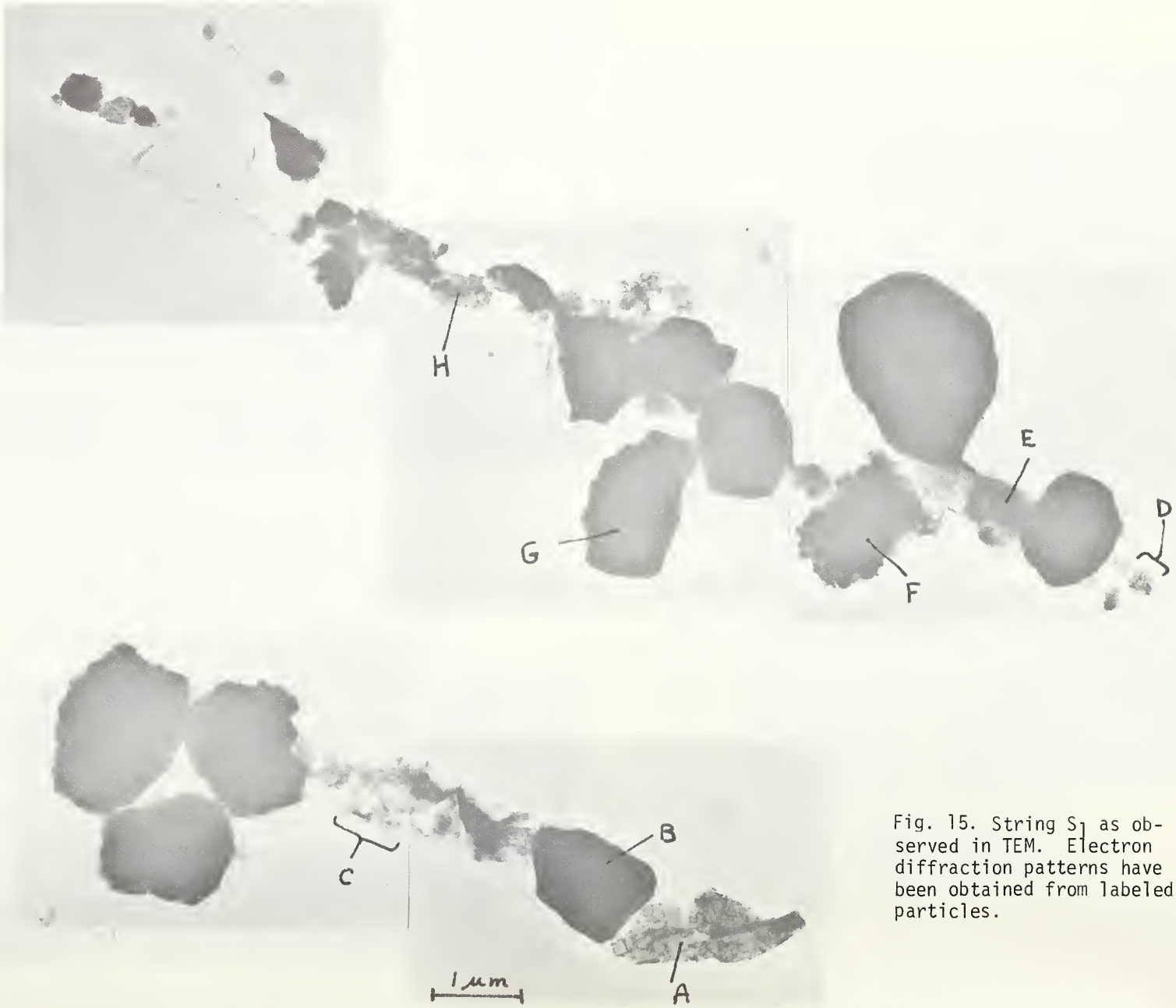

Fig. 15. String S_1 as observed in TEM. Electron diffraction patterns have been obtained from labeled particles.

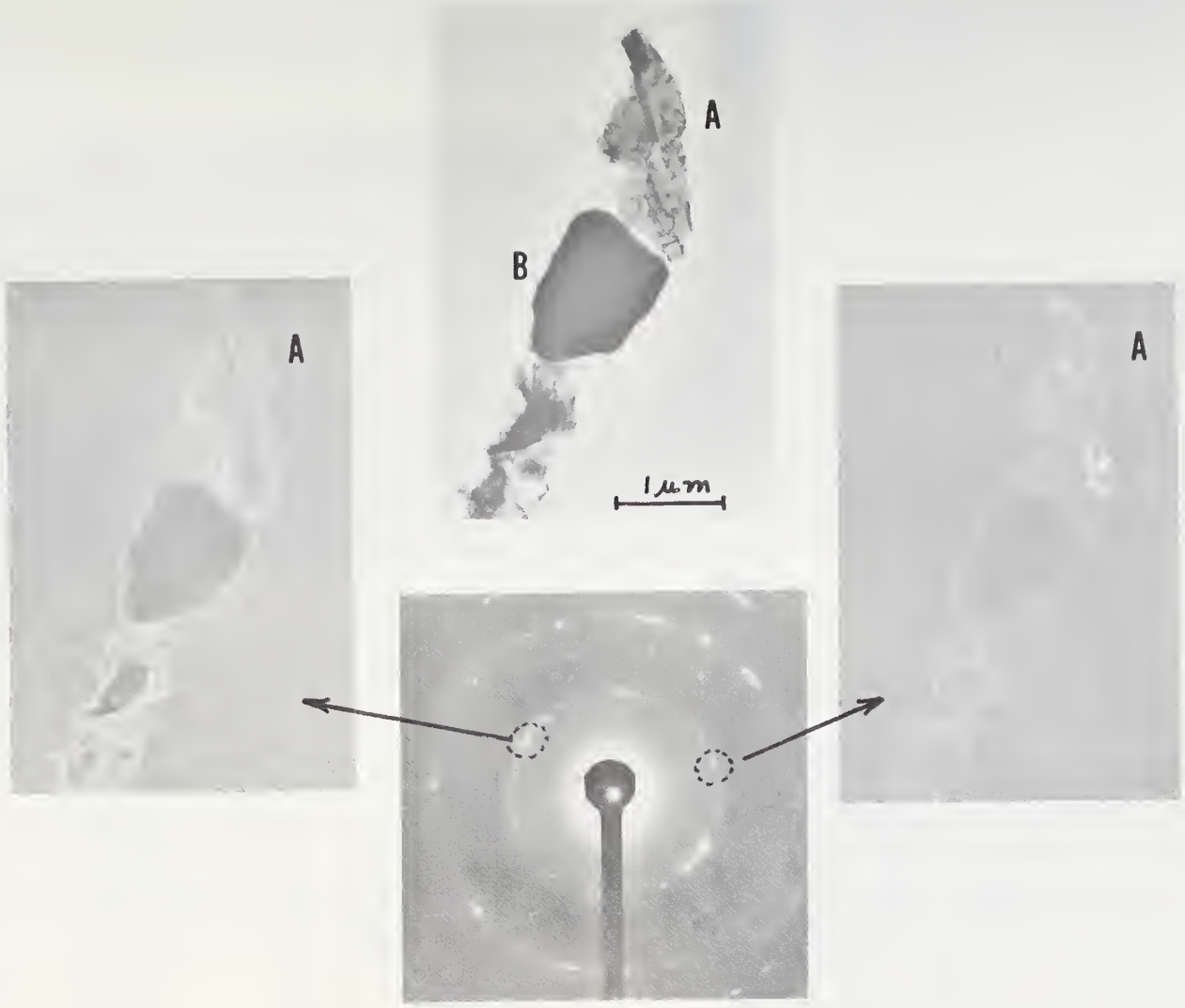

Fig. 16. Particles in string S_1 imaged in TEM bright field and two dark field reflections (iron and iron oxide). Note oxide covering at edge of opaque iron particle.

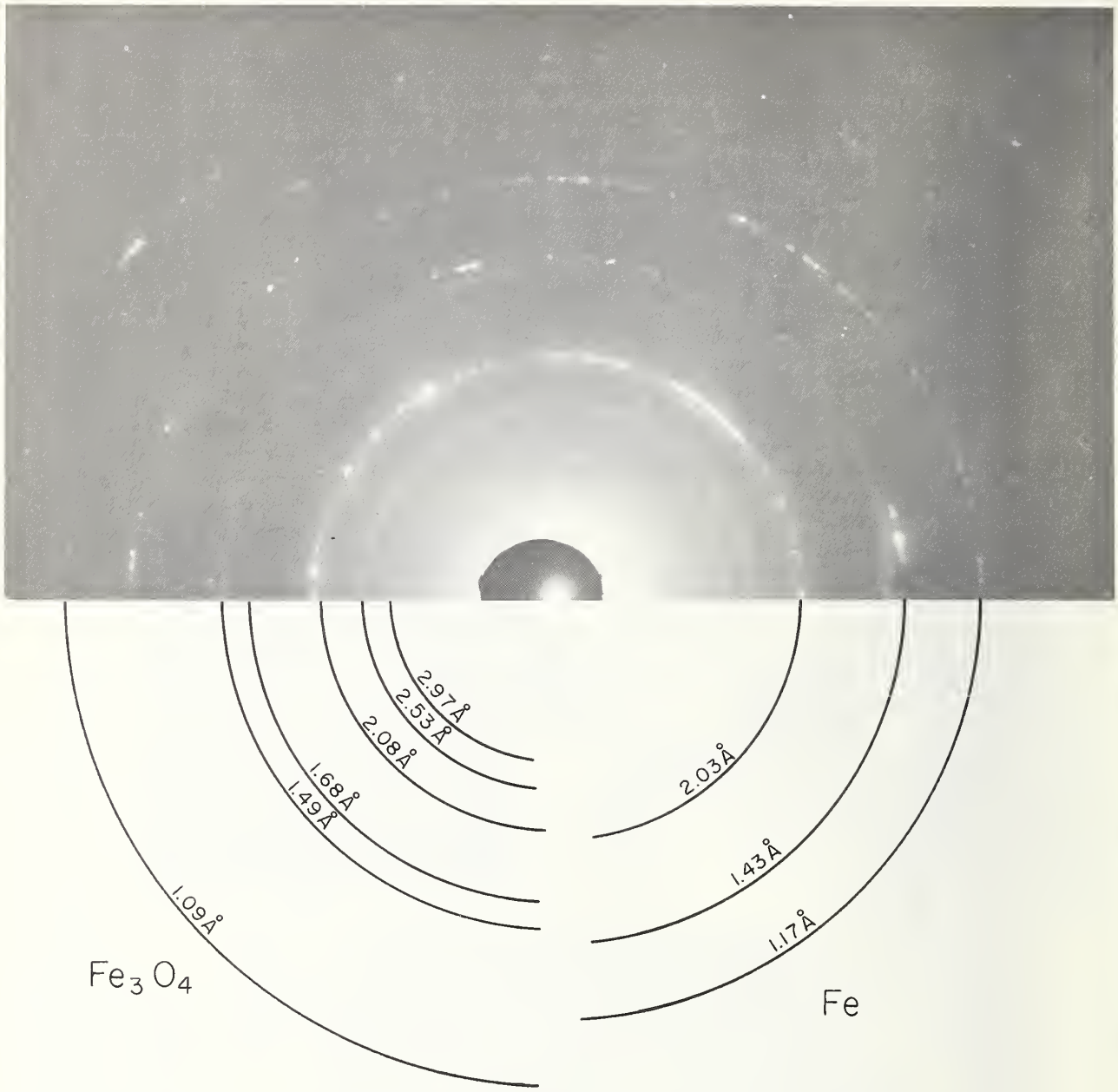

Fig. 17. Electron diffraction pattern from an area of partially oxidized iron particles in one string. F-1851.

Fig. 18. String S_2 in SEM. Note contrast difference among particles. M = 11,000x.

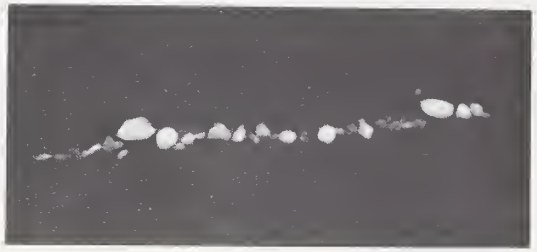

F-1851. String S_2 observed in SEM. M = 2,200x.

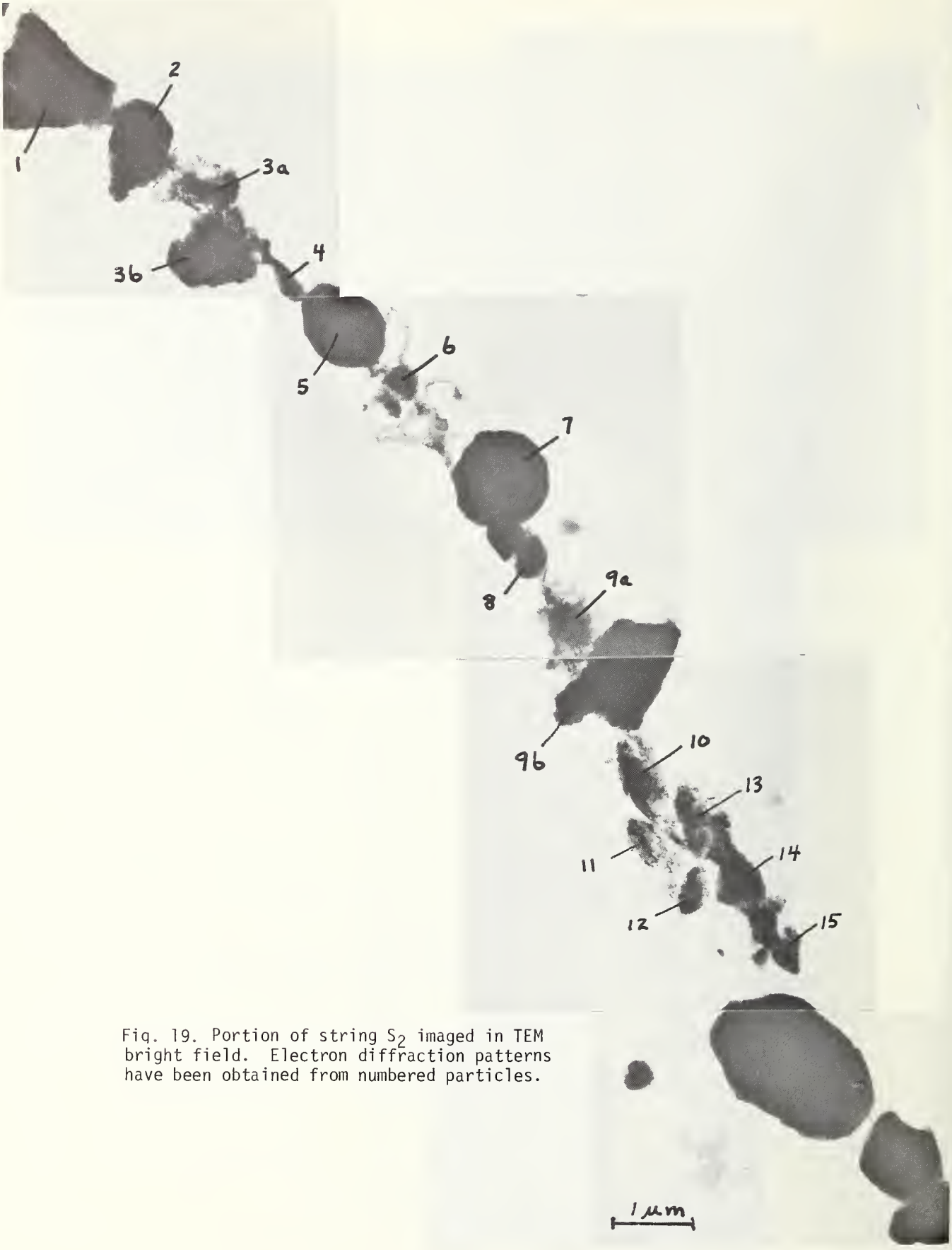

Fig. 19. Portion of string S_2 imaged in TEM bright field. Electron diffraction patterns have been obtained from numbered particles.

Fig. 20. Ferrogram 2119 from single ball test run. Initial particle deposit is at C. Flow is downward. M = 100x.

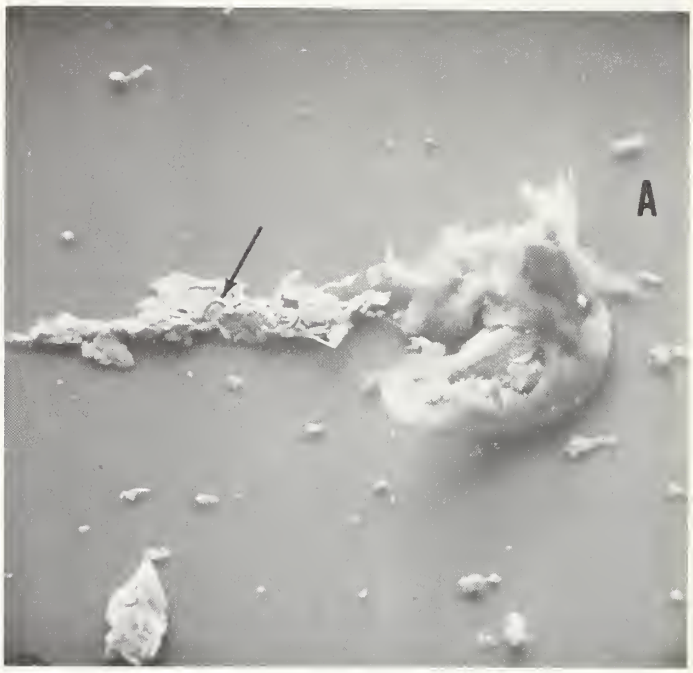

Fig. 21(a). Region A from above shows string containing flake-like particles and several examples of ribbon-like particles. M = 500X.

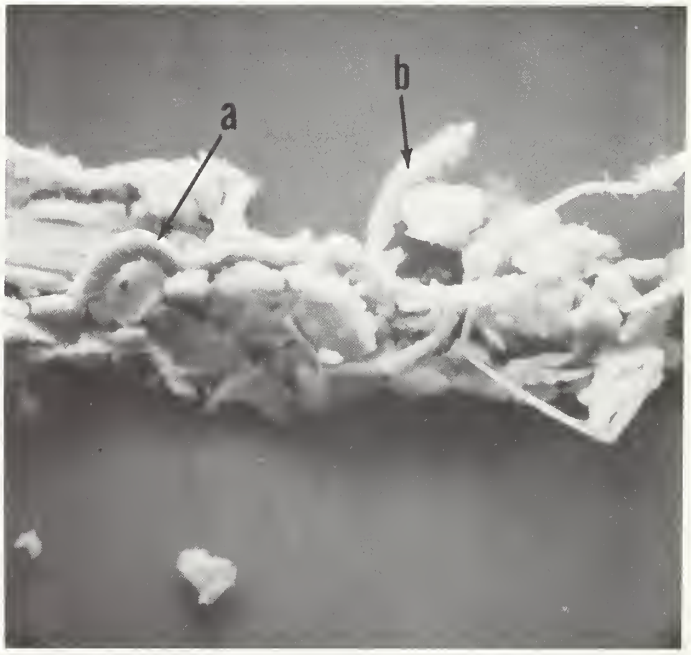

(b). Details of ribbon-like particles in above string. Note apparent deformation markings on ribbon (a). Both ribbons indicated are alloy steel with principal elements Fe(9,300 cts), Cr(3,200 cts) and Ni(1,000 cts). Ribbon (b) also contains Cu. M = 2,000X.

Fig. 22(a). Region B from above. Several small particle strings are present. M = 500X.

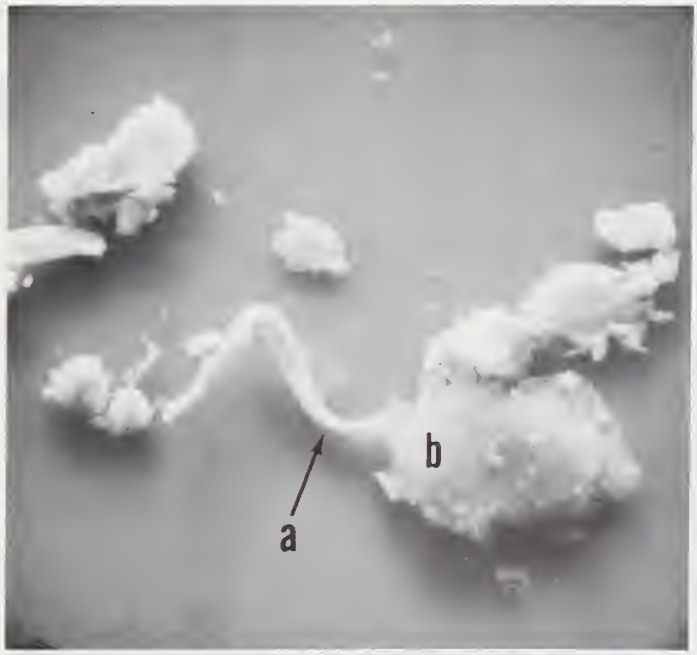

(b). Details of ribbon-like particle in above string (a), containing Fe, Cr, and Ni. Blob (b) contains only Fe, about 40% that of (a) plus oil residue and is probably iron oxide. M = 2,000X.

Fig. 23(a). Particle strings in Region C of above. Flake and ribbon-like particles and one spheroid (arrow) are seen. M = 300X.

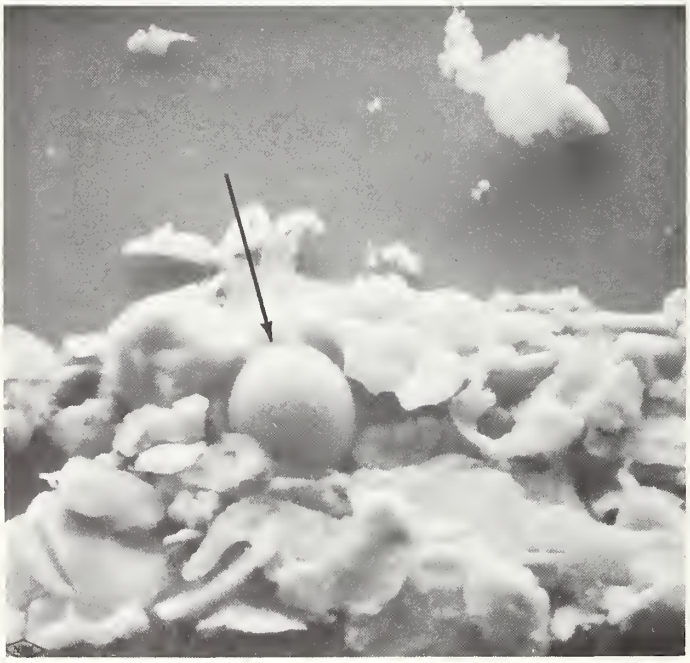

(b). Details of above string and spheroidal particle of 8 μm diameter. M = 2,000X.

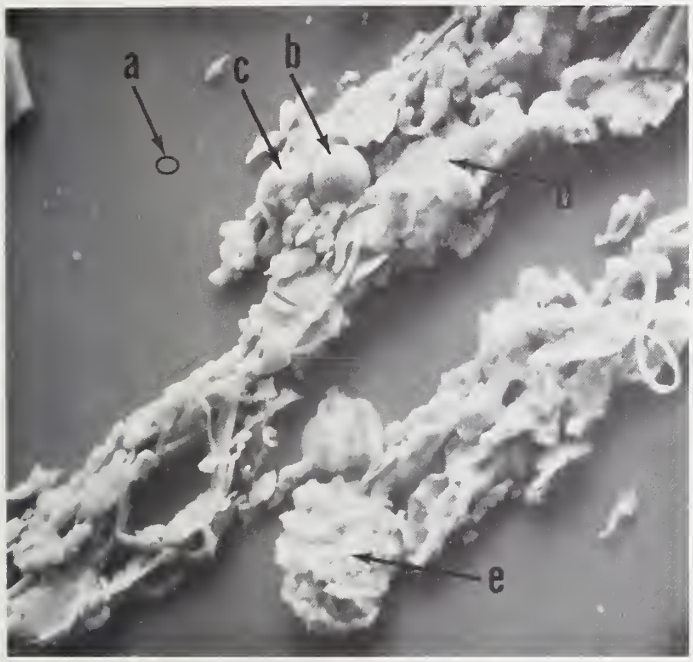

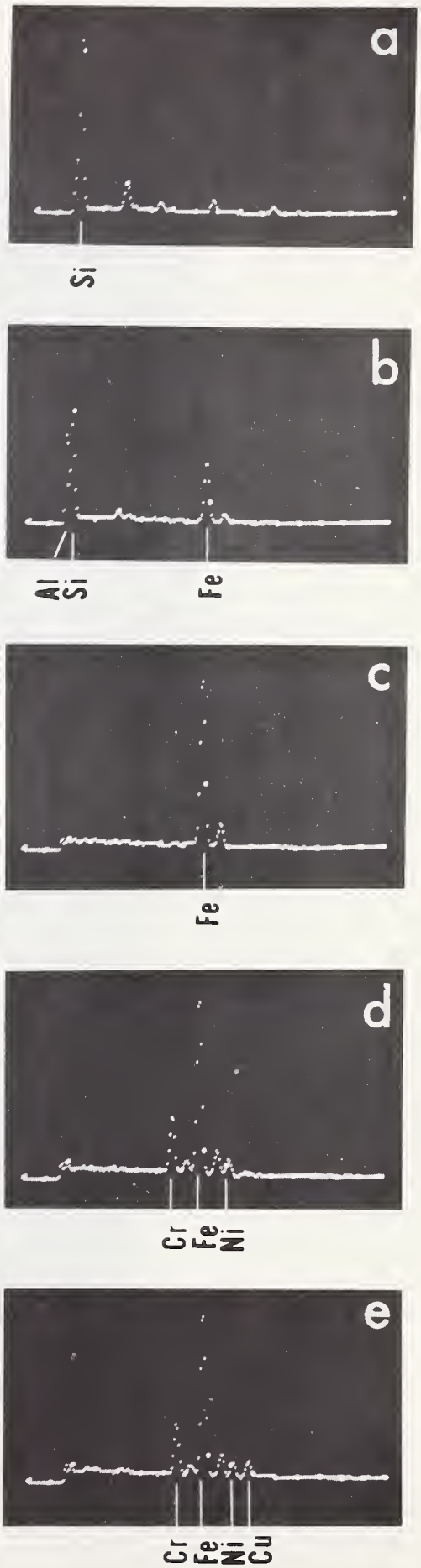

Fig. 24. Area of above with X-ray emission analyses shown for labeled particles and background (a). Spheroidal particle (b) has considerable Si, Al, and Fe content. Particle (c) is principally iron while particle (d) has substantial Cr and Ni content indicating alloy steel particle. Particle (e) contains Cu in addition. M = 1,000X.

Fig. 25(a). Surface of bearing ball, 11/16 inch diameter, 52100 steel, after bearing bench test. Wear and gouge tracks are seen in SEM photo. M = 3,000x.

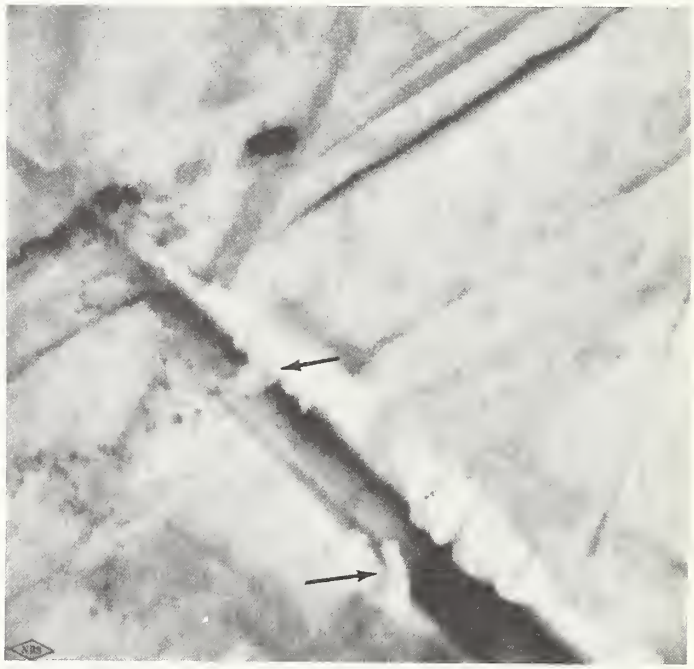

(b). Details of metal deformed over gouge rim. Several particles appear to be forming. M = 12,000x.

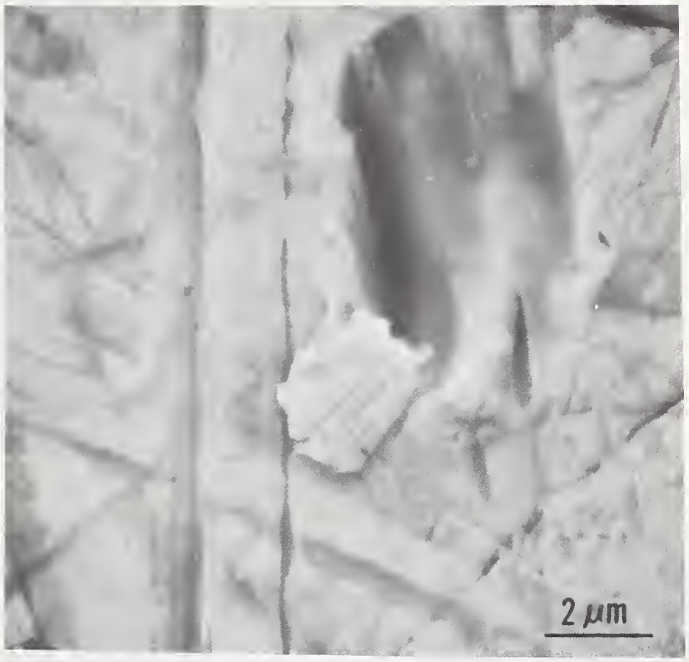

Fig. 26. Particle formed at edge of gouge on ball surface. Note surface wear markings on particle. M = 7,000x.

Fig. 27(a). Surface spall on ball from failed bearing. M = 60x.

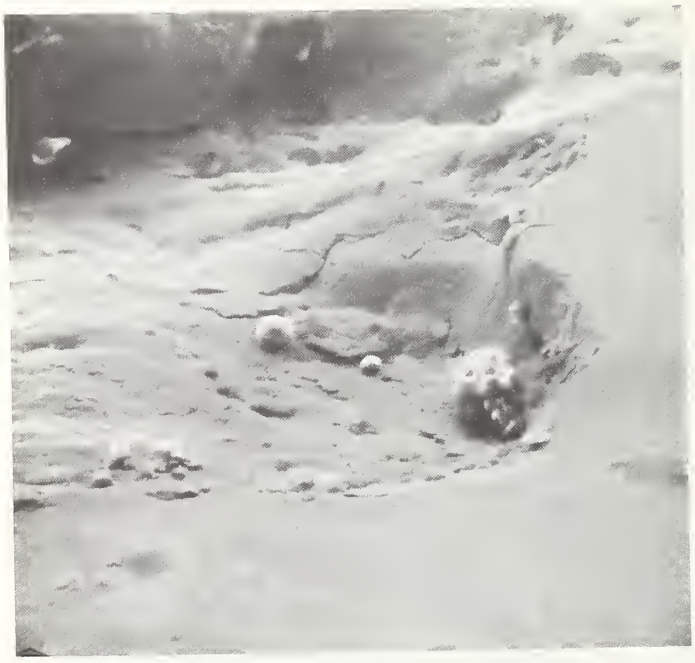

(b). Edge of above spall showing fracture surface features and spheroidal particles on surface. M = 240x.

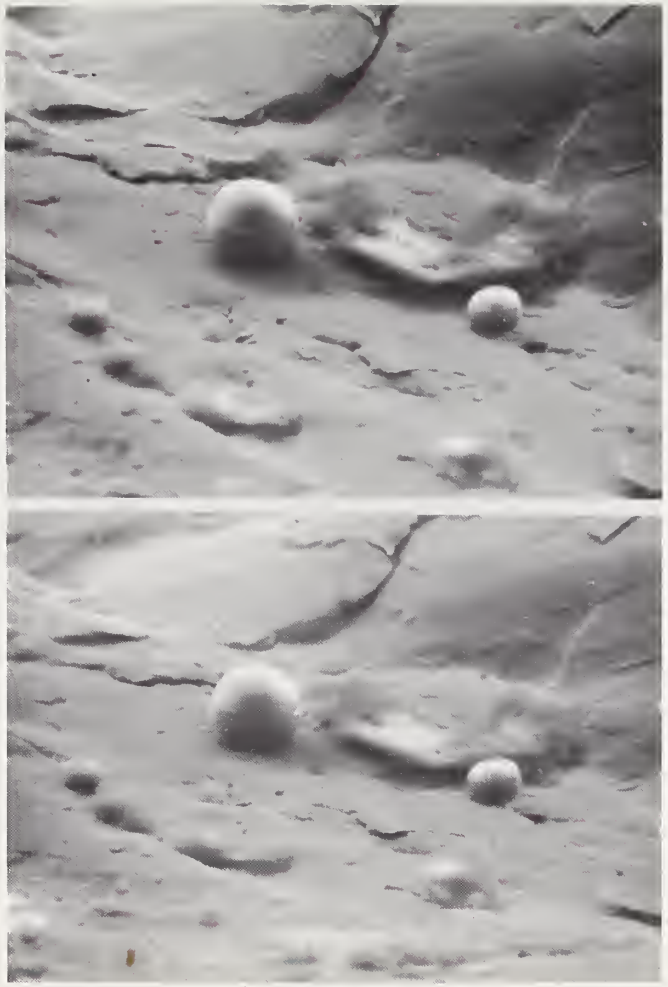

Fig. 28. SEM stereo photographs of above spheroidal particles on spall surface. Upper and lower views form right-left stereo pair, respectively. M = 600x.

DISTRIBUTION LIST

	NO. OF COPIES
Office of Naval Research Arlington, Virginia 22217 Attn: Code 411, R. S. Miller	1
Office of Naval Research Contract Administrator, Southeastern Area 2110 G Street, N.W. Washington, D. C. 20037	1
Director Naval Research Laboratory Washington, D. C. 20375 Attn: Technical Information Division	6
Code 2029	6
Defense Documentation Center Building 5 Cameron Station Alexandria, Virginia 22314	12
Air Force Materials Lab Wright-Patterson Air Force Base Dayton, Ohio 45433 Attn: Mr. F. Brooks	1
Department of Mechanical Engineering University of Virginia Charlottesville, Virginia 22091 Attn: P. Allaire	1
Department of Mechanical Engineering Chico State College Chico, California Attn: C. W. Allen	1
NASA-Lewis Research Center 21000 Brookpark Road Cleveland, Ohio Attn: W. J. Anderson	1
U. S. Steel Corporation Applied Research Lab Mailing Station 63 Monroeville, Pa. 15146 Attn: C. A. Bailey	1
Esso Research and Engineering Co. P.O. Box 51 Linden, New Jersey 07036 Attn: A. Brenbower	1

Mechanical Engineering Department
Massachusetts Institute of Technology
Cambridge, Mass. 02139
Attn: B. G. Bightmire 1

E. E. Bisson 1
20706 Eastwood Avenue
Fairview Park, Ohio 44126

Sibley School of Mechanical Engineering
Cornell University
Ithaca, New York 14850
Attn: J. E. Booker 1

Westinghouse Research Labs
Beulah Road
Churchill Boro
Pittsburgh, Pa. 15235
Attn: P. H. Bowen 1

Department of Mechanical Engineering
Georgia Institute of Technology
Atlanta, Georgia 30332
Attn: J. M. Bradford 1

General Electric Company
Silicon Products Department
Waterford, New York
Attn: E. D. Brown, Jr. 1

Naval Research Laboratory
Washington, D. C. 20375
Attn: R. C. Bowers, Code 6050 1

NASA-Lewis Research Center
21000 Brookpark Road
Cleveland, Ohio 44135
Attn: D. A. Buckley 1

Department of Mechanical Engineering
and Astronautical Sciences
Northwestern University
Evanston, Illinois 60201
Attn: H. S. Cheng 1

Maar Sciences Inc.
32 Sutherland Drive
Scotia, New York 12302
Attn: H. Campbell 1

Xerox Corporation
701 S. Aviation
El Segundo, California 90245
Attn: S. Chai 1

Department of Mechanical Engineering
and Astronautical Sciences
Northwestern University
Evanston, Illinois 60201
Attn: R. A. Burton 1

Institute of Fluid Mechanics
Academy of the Socialist Republic Rumania
Bucharest, Rumania
Attn: V. N. Constantinescu 1

John Deere Waterloo Tractor Works
Waterloo, Iowa 50704
Attn: P. K. Das 1

Aero Material Department
Naval Air Development Center
Johnsville, Warminster, Pa. 18974
Attn: M. J. Devine 1

Office of Naval Research
Arlington, Virginia 22217
Attn: S. Doroff 1

Virginia Polytechnic Institute
Blacksburg, Virginia 24061
Attn: N. S. Eiss, Jr. 1

Department of Mechanical Engineering
Columbia University
New York, New York
Attn: H. G. Elrod 1

IBM Corporation
Systems Products Division
Endicott, New York 13760
Attn: P. A. Engel 1

Fundamental Research Section
Research and Technical Department
Texaco Research Center
Beacon, New York
Attn: R. Fein 1

Mechanical Engineering Department
Virginia Polytechnic and State Univ.
Blacksburg, Virginia 24061
Attn: M. Furey 1

Naval Air Development Center
Johnsville, Warminster, Pa. 18974
Attn: M. K. Gabel 1

Chevron Research Company
576 Standard Avenue
Richmond, California 94800
Attn: D. Godfrey 1

Department of Mechanical Engineering
University of Virginia
Charlottesville, Va. 22091
Attn: E. J. Gunter 1

Mechanical Development Department
Research Laboratories
General Motors Corporation
Warren, Michigan 48090
Attn: D. F. Hays 1

Department of Machine Design
Technical University of Denmark
DK-2800 Lyngby, Denmark
Attn: J. Jakobsen 1

Department of Mechanical Engineering
University of Virginia
Charlottesville, Va. 22091
Attn: W. Jamaison 1

NASA-Lewis Research Center
21000 Brookpark Road
Cleveland, Ohio 44135
Attn: R. L. Johnson 1

University of Virginia
Thornton Hall
Charlottesville, Va. 22091
Attn: J. J. Kauzlarich 1

Cincinnati, Inc.
P.O. Box 11111
Cincinnati, Ohio 45211
Attn: R. A. Ketterer 1

Mechanical Engineering Department
Texas A&M University
College Station, Texas
Attn: D. F. Kettlebourgh 1

Department of Chemical Engineering
Pennsylvania State University
University Park, Pa. 16802
Attn: E. E. Klaus 1

Director, Department of Aerospace
Properties Research
Southwest Research Institute
8500 Culebra Road
San Antonio, Texas 78206
Attn: P. M. Ku 1

Department of Mechanical Engineering
Cleveland State College
Cleveland, Ohio
Attn: V. H. Larson 1

Department of Mechanics
Rensselaer Polytechnic Institute
Troy, New York 12181
Attn: F. F. Ling 1

Timken Company
1835 Dueber Avenue, S.W.
Canton, Ohio 44706
Attn: W. E. Littmann 1

Department of Mechanical Engineering
University of Michigan
Ann Arbor, Michigan 48105
Attn: K. Ludema

Department of Engineering Mechanics
North Carolina State University
Raleigh, N. C. 27607
Attn: C. J. Maday 1

Ford Motor Company
Research Laboratory
Dearborn, Michigan 48120
Attn: J. Meyer 1

Mobil Research & Development Corp.
Central Research Division
Box 1025
Princeton, N.J. 08540
Attn: W. R. Murphy 1

National Science Foundation
Engineering Mechanics Division
1800 G Street
Washington, D. C.
Attn: H. S. Ojalvo 1

Shaker Research, Inc.
Latham, New York 12110
Attn: C. T. Pan 1

NASA-Lewis Research Center
21000 Brookpark Road
Cleveland, Ohio 44135
Attn: R. Parker 1

Wear Sciences, Inc.
32 Sutherland Drive
Scotia, New York 12302
Attn: M. B. Peterson 1

Mechanical Engineering Department
Cornell University
Ithaca, New York 15850
Attn: R. M. Phelan 1

Mobil Research & Development Corp.
Box 1025 Princeton, New Jersey 08540
Attn: C. N. Rowe 1

Department of Mechanical Engineering
Georgia Institute of Technology
Atlanta, Georgia 30332
Attn: D. M. Sanborn 1

Department of Materials Engineering
University of Illinois at Chicago Circle
Box 4348
Chicago, Illinois 60680
Attn: J. A. Schey 1

University of Wisconsin
1513 University Avenue
Madison, Wisconsin 53706
Attn: A. Seireg 1

Mechanical Engineering Department
Carnegie-Mellon University
Pittsvurgh, Pa.
Attn: M. C. Shaw 1

Maic Division
Pure Carbon Co., Inc.
St. Marys, Pa. 15857
Attn: J. J. Sherlock 1

Pratt & Whitney Aircraft (MS-EB2B)
400 Main Street
East Hartford, Conn.
Attn: R. P. Sevchenko 1

SKF Industries, Inc.
1100 First Avenue
King of Prussia, Pa. 15857 1
Attn: L. B. Sibley

Mechanical Engineering Department
University of Tennessee
Knoxville, Tennessee 37916
Attn: K. Stair 1

Ford Motor Company
Research Laboratory
Dearborn, Michigan 48120
Attn: L. Ting 1

General Electric Company
Building 55-119
Schenectady, N.Y. 12305
Attn: J. H. Vohr 1

Manager, Bearings, Lubrication
& Seals
Mechanical Technology, Inc.
968 Albany Shaker Road
Latham, New York 12110
Attn: D. F. Wilcock 1

Department of Mechanical Engineering
Georgia Institute of Technology
Atlanta, Georgia 30332
Attn: W. O. Winer 1

NASA-Lewis Research Center
21000 Brookpark Road
Cleveland, Ohio 44135
Attn: E. V. Zaretsky 1

Office of Naval Research
Arlington, Virginia 22217
Attn: P. Clarkin, Code 471 1
K. Ellingsworth, Code 473 1

Naval Ship Engineering Center
Prince George's Center
Hyattsville, Maryland 20782
Attn: L. B. Hebbard, Code 6107 1
R. Lane, Code 6101F 1

Naval Air Systems Command
Washington, D. C. 20360
Attn: B. Poppert, Code 340E 1
E. Regelson, Code 4115 1
H. Rosenwasser, Code 424 1

Chief of Naval Material
Washington, D. C. 20360
Attn: CAPT W. Holton, Code 041 1
CAPT G. D. Webber, Code 09H 1
J. Ward, 04112 1

Naval Air Engineering Center
Ground Support, Equipment Division
Philadelphia, Pa. 19112
Attn: Code SE-624, P. Senholze 1

Naval Ship Research and Development Laboratory
Annapolis, Maryland 21401
Attn: Mr. N. Glassman, Code 821 1
Mr. W. Smith, Code 2832 1

Air Force Aero Propulsion Laboratory
AFAPL/SFL
Wright Patterson Air Force Base, Ohio 45433
Attn: Mr. C. Hudson 1

National Engineering Laboratory
East Kilbridge, Glasgow (G. Britain)
Attn: Mr. D. Scott 1

National Bureau of Standards
Department of Commerce
Washington, D. C. 20234
Attn: Dr. E. Passaglia 1
Dr. W. Ruff 1

Institute of Ocean Science & Engineering
Dept. of Civil & Mechanical Engineering
The Catholic University of America
Washington, D. C. 20017
Attn: Dr. A. Thiruvengadam 1

U. S. Army Mobility Equipment Command
Directorate of Research, Development and Engineering
Fort Belvoir, Virginia 22060
Attn: Mr. A. J. Rutherford 1

Office of Secretary of Defense (I&L)
The Pentagon, Room 2B322
Washington, D. C. 20350
Attn: Mr. H. Peterson 1

AFSME Oil Analysis Section
Room 4A264, The Pentagon
Washington, D. C. 20350
Attn: COL Benjamin 1

University College of Swansea
Singleton Par,
Swansea, Wales SA28PP
Attn: Prof. F. T. Barwell 1

Massachusetts Institute of Technology
Lincoln Laboratory
Cambridge, Mass. 02139
Attn: Prof. N. Cook 1
Prof. E. Rabinowicz 1
Prof. N. Suh 1

Imperial College of Science and Technology
Dept. of Mechanical Engineering
Exhibition Road
London, England SW7
Attn: Prof. Alistair Cameron 1

AB-SVENSKA KULLAGERFABRIKEN
Group Headquarters
S-41550
Gothenberg, Sweden
Attn: Dr. A. Palmgren 1

Mr. Robert Q. Barr 1
Associate Director
Technical information
Climax Molybdenum Company
1270 Avenue of Americas
New York, N.Y. 10020

Commander
Naval Ships Systems Command
Code 045N
Washington, D. C. 20362 1

Naval Ordnance Systems Command
Code 0442
Washington, D. C. 20360
Attn: G. Tsuchida 1

Naval Ordnance Systems Command
Code ORD-04531
Washington, D. C. 20360
Attn: A. R. Romano 1

Naval Ordnance Systems Command
Washington, D. C. 20360
Attn: CDR F. Jonasz 1

Naval Ordnance Station
Code 50331
Louisville, Kentucky 40214
Attn: J. W. Patton 1

Quality Evaluation and Engineering Laboratory
NAD/Oahu (Code 3032)
FPO San Francisco 96612
Attn: Seiji Sakata 1

Commander
Cruiser Destroyer Force,
Atlantic Fleet
Code 414
Norfolk, Virginia 23511
Attn: FTCS Buchanan 1

Commander
Cruiser Destroyer Force,
Pacific Fleet
Code 434
San Diego, California 92110
Attn: Chief Collins 1

Commanding Officer
Naval Ordnance Systems Support Office, Atlantic
Building #62
Norfolk Naval Shipyard
Portsmouth, Va. 23709
Attn: J. Reidy 1

Commanding Officer
Naval Ordnance Systems Support Office, Pacific
Post Office Box 80548
San Diego, California 92138
Attn: Code 081 Clay Westfall 1

Commanding Officer
Naval Ship Engineering Center
Code 6101F
Prince George's Center
Hyattsville, Maryland 20782
Attn: E. C. Davis 1

Commanding Officer
Naval Air Rework Facility
Technical Support Center
Code 360
Naval Air Station
Pensacola, Fla. 32508
Attn: R. Purcell 1

Commander
Charleston Naval Shipyard
Metals Section,
Material Laboratory
Code 131.11
Charleston, S. C. 29408
Attn: Hillary Douglas 1

Commander
Naval Ship Repair Facility
Subic
FPO San Francisco 96612 1

Commander
Naval Ship Repair Facility
Guam
FPO San Francisco 96612 1

Department of Chemistry
University of North Carolina
Chapel Hill, N.C. 27514
Attn: Dr. T. Isenhower 1

NBS-114A (REV. 7-73)

U.S. DEPT. OF COMM. BIBLIOGRAPHIC DATA SHEET	1. PUBLICATION OR REPORT NO. NBSIR 74-474	2. Gov't Accession No.	3. Recipient's Accession No.

4. TITLE AND SUBTITLE	5. Publication Date
Metallurgical Analysis of Wear Particles and Wearing Surfaces	April 1974
	6. Performing Organization Code
7. AUTHOR(S) A. W. Ruff	8. Performing Organ. Report No.
9. PERFORMING ORGANIZATION NAME AND ADDRESS NATIONAL BUREAU OF STANDARDS DEPARTMENT OF COMMERCE WASHINGTON, D.C. 20234	10. Project/Task/Work Unit No. 3120108
	11. Contract/Grant No. NA ONR-31-73
12. Sponsoring Organization Name and Complete Address (Street, City, State, ZIP) Department of the Navy Office of Naval Research Arlington, Virginia 22217	13. Type of Report & Period Covered April 73 - April 74 Final Report
	14. Sponsoring Agency Code

15. SUPPLEMENTARY NOTES

16. ABSTRACT *(A 200-word or less factual summary of most significant information. If document includes a significant bibliography or literature survey, mention it here.)*

Results are presented from a program involved in characterizing the wear particles and surface degradation produced by wear in bearing and gear tests in which the effects of several variables on failure of the wearing surfaces has been examined. The information obtained has been correlated with the results of allied studies conducted by others in an attempt to develop an understanding of the processes producing wear and degradation of metal surfaces in sliding, rubbing, rolling, and/or rotating contact and the effects of lubricants, lubricant additives, bearing materials etc. on these processes. The characterization of the wear particles and wearing surfaces should aid in the establishment of the interrelationships between wear particle shape, size, size distribution, chemical compositions, metallurgical structure, and surface damage prior to failure.

17. KEY WORDS *(six to twelve entries; alphabetical order, capitalize only the first letter of the first key word unless a proper name; separated by semicolons)*

Bearings; Electron diffraction; Electron microscopy; Gears; Lubrication; Particles; Wear

18. AVAILABILITY	19. SECURITY CLASS (THIS REPORT)	21. NO. OF PAGES
[XX] Unlimited	UNCLASSIFIED	30
[ ] For Official Distribution. Do Not Release to NTIS		
[ ] Order From Sup. of Doc., U.S. Government Printing Office Washington, D.C. 20402, SD Cat. No. C13	20. SECURITY CLASS (THIS PAGE)	22. Price
[ ] Order From National Technical Information Service (NTIS) Springfield, Virginia 22151	UNCLASSIFIED	

USCOMM-DC 29042-P74

AMERICAN REVOLUTION BICENTENNIAL
1776-1976